Beni-Suef University Journal of Basic and Applied Sciences

RESEARCH

Open Access

Computational elucidation of the potential mechanisms of *Warburgia ugandensis* against colorectal cancer

Yohana Amos[1,2*], Bienvenu Nsengimaana[3*], Mercy Bisola Faleyimu[4], Peter Olorundunsin Adeniyi[5,6], Aishat Adebola Lawal[7], Orace Mathieu Kenou[8], Darius Riziki Martin[9,10], Ashita Jawali[11] and Olaitan I. Awe[12,13*]

Abstract

Background Colorectal cancer remains a major global health challenge due to its high incidence, mortality, therapeutic resistance, and treatment-related adverse effects. *Warburgia ugandensis* is a medicinal plant that has demonstrated anti-colorectal cancer; however, the specific bioactive compounds responsible and their underlying molecular mechanisms remain underexplored. This study investigated the anti-colorectal cancer potential and molecular mechanisms of *W. ugandensis* phytochemicals using an integrated computational approach.

Methods Phytochemicals were retrieved from published literature and the Collection of Open Natural Products database, standardized, and screened for drug-likeness and oral bioavailability. Potential protein targets were predicted and intersected with colorectal cancer-associated genes, followed by network pharmacology and functional enrichment analyses. Molecular docking, 100 ns molecular dynamics simulations, molecular mechanics Poisson-Boltzmann surface area binding energy calculations, and absorption, distribution, metabolism, excretion, and toxicity (ADMET) analyses were performed to evaluate compound-target interactions, complex stability, and pharmacological properties.

Results Among 242 identified phytochemicals, 21 compounds satisfied drug-likeness and oral bioavailability criteria. Target prediction identified 435 potential protein targets of the screened phytochemicals, of which 411 overlapped with colorectal cancer-associated genes. Network analysis of the overlapping targets identified PIK3CA, PIK3CD, GNAI1, GNAI3, and SRC as key hub genes. Functional enrichment analysis suggested that these targets are involved in cancer-relevant signaling pathways, including the phosphatidylinositol 3-kinase-protein kinase B, insulin receptor, and relaxin signaling pathways. Molecular docking identified quercetin, kaempferol, and bemadienolide as leading candidates, with strong binding affinities toward GNAI1 (-9.8 kcal/mol), GNAI3 (-9.6 kcal/mol), and PIK3CD (-8.7 kcal/mol), respectively. Molecular dynamics simulations demonstrated stable protein-ligand complexes with reduced

*Correspondence:
Yohana Amos
yohanaamos021@gmail.com
Bienvenu Nsengimaana
bienvenunsengimaana@gmail.com
Olaitan I. Awe
laitanawe@gmail.com

Full list of author information is available at the end of the article

Springer Open

© The Author(s) 2026. **Open Access** This article is licensed under a Creative Commons Attribution-NonCommercial-NoDerivatives 4.0 International License, which permits any non-commercial use, sharing, distribution and reproduction in any medium or format, as long as you give appropriate credit to the original author(s) and the source, provide a link to the Creative Commons licence, and indicate if you modified the licensed material. You do not have permission under this licence to share adapted material derived from this article or parts of it. The images or other third party material in this article are included in the article's Creative Commons licence, unless indicated otherwise in a credit line to the material. If material is not included in the article's Creative Commons licence and your intended use is not permitted by statutory regulation or exceeds the permitted use, you will need to obtain permission directly from the copyright holder. To view a copy of this licence, visit http://creativecommons.org/licenses/by-nc-nd/4.0/.

structural fluctuations over 100 ns. Binding free energy analysis revealed favorable interactions, with quercetin-GNAI1 showing the strongest predicted binding stability (-86.2 ± 3.3 kcal/mol). Pharmacokinetic and toxicity predictions indicated high gastrointestinal absorption and generally low predicted toxicity profiles.

Conclusion This study provides computational, hypothesis-generating evidence that *Warburgia ugandensis* phytochemicals may modulate multiple molecular targets and signaling pathways involved in colorectal cancer. Quercetin, kaempferol, and bemadienolide represent promising candidates for further experimental investigation. Nevertheless, these predictive findings require validation through in-vitro and in-vivo studies to establish their therapeutic relevance.

Clinical trial number Not applicable.

Keywords Colorectal cancer, *Warburgia ugandensis*, Phytochemicals, Network pharmacology, Molecular modelling

1 Introduction

Colorectal cancer (CRC) represents a significant global health burden, being the third most commonly diagnosed cancer and the second leading cause of cancer-related mortality worldwide [1, 2]. Each year, CRC accounts for over 1.8 million cases and more than 860,000 fatalities, with incidence and mortality varying across populations; the lowest rates are observed among Asian Americans and Pacific Islanders, whereas non-Hispanic Blacks exhibit the highest [3–5]. Men are 30–40% more likely than women to develop CRC. CRC prevalence globally is anticipated to rise by more than 60% in the coming decades [6, 7], highlighting the critical need for effective prevention and treatment approaches. Lifestyle factors such as physical inactivity, alcohol consumption, obesity, red or processed meat intake and smoking increase CRC risk, whereas adherence to a healthy diet, regular exercise, and weight control can minimize risk by up to 37% [4, 8, 9].

At the molecular level, CRC arises through deregulation of multiple interconnected signaling pathways that control cell cycle, differentiation, apoptosis, and metastasis [10]. Alterations in the APC gene activate the Wnt/β-catenin signaling cascade, leading to unregulated cell propagation [11], while dysregulation of the PI3K/AKT/mTOR, MAPK/ERK, and p53/Bcl-2 cascades promote survival and confer apoptosis resistance [12–14]. Aberrant activation of TGF-β/SMAD, Notch, and JAK/STAT signaling drives epithelial-mesenchymal transition (EMT), enhances invasive potential, and sustains cancer stemness traits, whereas chronic NF-κB and COX-2 activation sustains inflammation, angiogenesis, and tumor progression. Metastasis, a hallmark of CRC, involves EMT-mediated cell detachment, extracellular matrix degradation by matrix metalloproteinases, vascular invasion, intravasation, survival in circulation, and colonization of distant organs, particularly the liver [15–20]. The dynamic interplay between these oncogenic and inflammatory cascades, together with the tumor microenvironment and gut microbiota, underlies CRC development and heterogeneity [21].

Current treatments for CRC include surgery, radiotherapy, chemotherapy, immune-based and targeted therapies (nivolumab, pembrolizumab, ipilimumab) [2, 22, 23]. While these approaches have improved survival, their effectiveness is often constrained by systemic toxicity, tumor diversity, chemoresistance, and recurrence [24]. Immune- and targeted-based therapies show benefits primarily in specific patient subgroups, such as those harboring tumors with high microsatellite instability (MSI-H) or deficient mismatch repair (dMMR), leaving many patients with suboptimal outcomes [25]. Such problems underscore the immediate need for innovative, safer, and more efficacious interventions that can modulate multiple oncogenic pathways simultaneously. In this regard, natural products and bioactive phytochemicals offer promising multi-targeted strategies, with the potential to complement standard therapies, overcome therapeutic resistance, and support the development of safer, more efficient treatment regimens [26].

Warburgia ugandensis (East African greenheart), a medicinal plant of the *Canellaceae* family, has long been used locally to treat infections, inflammation, gastrointestinal disorders, rheumatism, fever, ulcers, and respiratory conditions [9, 27–29]. Phytochemical studies have reported flavonoids, tannins, sesquiterpenoids, and neolignanamides as key bioactive compounds mediating its pharmacological effects, including activation of CASP9 alongside reduced expression level of COX-2, 5-LOX, Bcl-xL, and Bcl-2, indicating anti-inflammatory and pro-apoptotic properties [9, 30, 31]. Despite these promising findings, a comprehensive evaluation of the phytocompounds of *W. ugandensis* responsible for its effects and their specific molecular targets in CRC remain underexplored. Therefore, the present study employs integrated in-silico approaches including network pharmacology, bioinformatics analysis, and molecular modeling to investigate the potential anti-CRC mechanisms of this plant. Specifically, the study seeks to identify key bioactive constituents, predict their potential protein targets, and elucidate the underlying signaling

pathways, thereby providing a scientific basis for future anticancer drug discovery and development.

2 Methods

All procedures are summarized in Fig. 1, depicting the overall workflow. Detailed methods are provided below.

2.1 Phytochemicals retrieval and screening

Phytocompounds from *Warburgia ugandensis* were collected through a systematic literature search and from the COCONUT database (COlleCtion of Open Natural prodUcTs, v.2022; accessed September 5, 2025) [32]. The dataset was curated in Python (v3.11) using pandas (v1.5.2). Standardization steps included conversion of

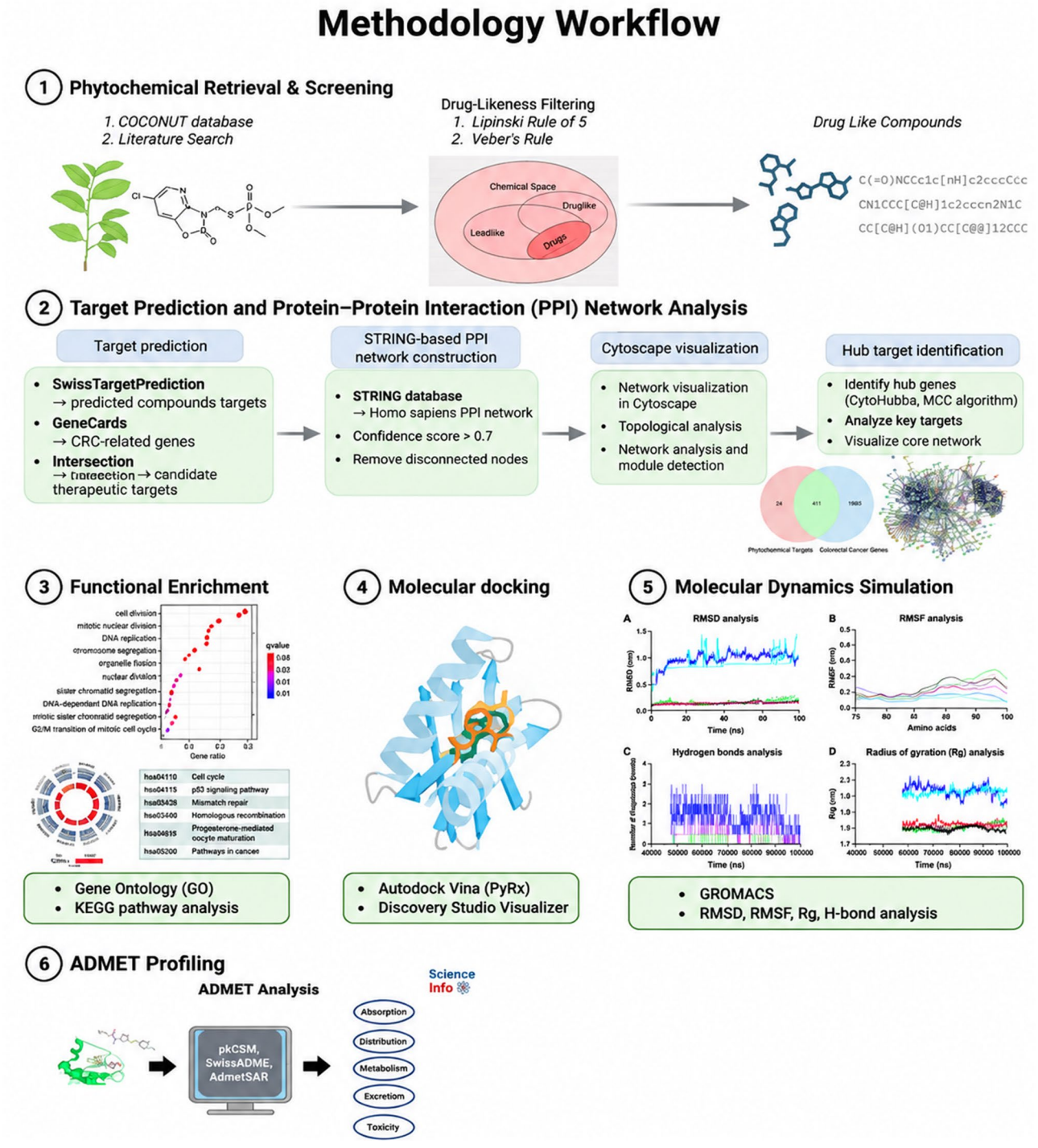

Fig. 1 Schematic workflow of the In-silico investigation of *Warburgia ugandensis* phytochemicals against colorectal cancer

compound names to uniform case, removal of extraneous characters and whitespace, replacement of Greek letters with textual equivalents, and elimination of duplicates via exact string matching. Canonical SMILES notations were obtained for each curated compound to enable downstream computational analyses. PubChem was queried programmatically using the PubChemPy library (v1.0.4). Compounds without exact matches were further searched using synonyms, similarity queries, or the ChEMBL REST API (v.32), and remaining unresolved compounds were retrieved directly from the COCONUT database. For each compound, canonical SMILES and database identifiers (PubChem CID, ChEMBL ID, or COCONUT ID) were recorded. Canonicalization ensured standardized tautomeric and stereochemical representations for all subsequent analyses.

Key molecular properties, including octanol/water distribution coefficient (LogP), molar refractivity (MR), molecular mass (MW), counts of hydrogen bond donors (HBD) and hydrogen bond acceptors (HBA), were calculated using RDKit (v2022.09.5). The compounds were evaluated according to an adapted Lipinski's Rule of Five (LogP ≤ 5, MW ≤ 500 Da, HBD ≤ 5, HBA ≤ 10, and MR between 40 and 130). Compounds meeting these criteria were subsequently screened using Veber's Rule to assess oral bioavailability, based on molecular polar surface area (TPSA ≤ 140 Å²) and flexible bond count (≤ 10) [33]. This filtering strategy was applied as a prioritization step to select compounds with predicted favorable oral bioavailability and drug-like pharmacokinetic properties. Only compounds satisfying both criteria were retained for downstream analyses.

2.2 Target gene prediction

The probable protein targets of the chosen phytochemicals were inferred using SwissTargetPrediction [34], which predicts targets based on the compound similarity to known ligands [35]. In addition, a post-hoc sensitivity check was run using SwissTargetPrediction's probability score (probability > 0.5). Canonical SMILES strings were used as input. Predicted targets were downloaded in CSV format. Genes associated with colorectal cancer (CRC) were retrieved from GeneCards by querying the term "*Colorectal Cancer*". Only protein-coding genes with established or predicted relevance to CRC were retained [36]. Non-protein-coding entries, including RNA genes, pseudogenes, functional elements, genetic loci, gene clusters, and uncategorized records, were excluded. Candidate therapeutic targets were identified by intersecting phytochemical targets with CRC-related genes using Venny 2.1 [37, 38].

2.3 Protein-protein interaction network analysis and hub gene identification

Protein-protein interactions (PPI) of the overlapping gene targets were analyzed via the STRING database version 12.0, restricting to human (*Homo sapiens*) and applying an interaction confidence threshold of 0.9 to ensure reliability [39]. The resulting networks, in which nodes represented proteins and edges indicated functional interactions, were curated to remove self-loops and isolated nodes, enhancing interpretability. Network visualization and further topological analyses were performed in Cytoscape (v3.10.3). The different roles of genes in the pathogenesis and progression of diseases have been a thing of investigation in multiple studies [40–43]. Key genes within the protein-protein interaction network were determined using the CytoHubba plugin, employing the Maximal Clique Centrality (MCC) method to evaluate and rank nodes according to their network centrality and degree of connectivity. From this analysis, the ten most highly interconnected genes, representing nodes with potentially critical biological roles, were chosen for further pathway enrichment studies.

2.4 Functional enrichment analysis

Functional annotation and pathway enrichment of hub genes were performed using the SRplot web server (https://bioinformatics.com.cn/en) with *Homo sapiens* as the reference. Functional enrichment analysis was conducted using Gene Ontology (GO) to classify the genes into molecular functions (MF), biological processes (BP), and cellular components (CC). In parallel, KEGG pathway enrichment was performed to determine the signaling cascades associated with the target genes [44]. Statistical significance was defined as an adjusted p-value ≤ 0.05 following correction with the Benjamini-Hochberg procedure. For downstream interpretation, the ten most enriched GO terms in each category and the ten KEGG pathways with the highest significance were selected [45].

2.5 Molecular docking

Molecular docking was performed to investigate the binding interactions between selected phytochemicals and colorectal cancer-related target proteins. The SDF structures of phytochemicals were retrieved from the PubChem database and converted into three-dimensional conformations using OpenBabel software. 5-Fluorouracil (5-FU) was used as a reference compound; it was retrieved from the PubChem database using Compound CID 3385. Ligand preparation was carried out using PyRx (v0.8), where hydrogen atoms were added, rotatable bonds were defined, and appropriate protonation states, tautomers, and bond orders were assigned at physiological pH (7.4). Gasteiger partial charges were calculated,

and all ligands were energy-minimized and saved in PDBQT format for subsequent docking studies [46].

Three-dimensional structures of the target proteins PIK3CD (5DXU), GNAI1 (5JS7), GNAI3 (8OY1), PIK3CA (7R9V), PIK3CB (4BFR), PIK3R1 (3I5R), PIK3R2 (2KT1), PIK3R3 (5ZUT), SRC (8BQ3), and GNAI2 (9K6L) were retrieved from the Protein Data Bank (PDB). All selected structures were experimentally resolved, ensuring high structural reliability for docking studies. Protein preparation was performed using BIOVIA Discovery Studio Visualizer (2025), including removal of water molecules, heteroatoms, and non-essential chains, followed by addition of polar hydrogen atoms, assignment of bond orders, and energy minimization to eliminate steric clashes and optimize structural geometry [47]. Binding site definition was based on the coordinates of co-crystallized ligands present in each protein structure, ensuring biologically validated and experimentally confirmed active site selection [48]. The receptor grid box for docking was centered on the native ligand binding pocket for each target, allowing accurate reproduction of physiologically relevant interactions. This ligand-guided approach ensured consistent and reliable identification of active sites across all protein-ligand systems.

Molecular docking was conducted using AutoDock Vina implemented within PyRx (v0.8) [49]. For all protein targets, the receptor grid box was centered on the co-crystallized ligand binding site, ensuring accurate reproduction of experimentally validated active pocket interactions. Grid box dimensions were individually defined for each protein according to the spatial extent of the binding cavity to ensure complete coverage of the active region while maintaining binding site specificity. Docking calculations were performed using an exhaustiveness parameter ranging from 8 to 16 to ensure adequate conformational sampling of ligand poses within the binding pocket. The AutoDock Vina scoring function was used to estimate binding affinities (kcal/mol), and ligand conformations were ranked based on the lowest binding energy and stability of interactions. The most favorable docked poses were selected for further analysis based on binding affinity and consistent interactions within the active site. The best-ranked protein-ligand complexes were further analyzed to characterize intermolecular interactions, including hydrogen bonding, hydrophobic interactions, π–π stacking, and van der Waals forces. Two-dimensional interaction diagrams were generated using BIOVIA Discovery Studio Visualizer (2025) to visualize binding interactions.

To validate the docking protocol, a redocking procedure was performed for all proteins with available co-crystallized ligands. Native ligands were extracted from the crystal structures and re-docked into the same binding sites using identical docking parameters. The reliability of the docking protocol was assessed by calculating the root-mean-square deviation (RMSD) between the experimentally observed ligand poses and the redocked conformations, with RMSD values ≤ 2.0 Å considered acceptable, confirming the accuracy and reproducibility of the docking methodology [50].

2.6 Molecular dynamics (MD) simulations

Docked protein-ligand assemblies were prepared using CHARMM-GUI and parameterized with the CHARMM36m force field. The systems were then solvated in a TIP3P water box and neutralized with 0.15 M Na^+ and Cl^- ions. After energy minimization, equilibration was performed in two phases, consisting of 125 ps under the NVT ensemble (constant number of particles, volume, and temperature) followed by 250 ps under the NPT ensemble (constant pressure and temperature) at 310 K. Molecular dynamics production simulations were carried out in GROMACS 2019 for 100 ns using periodic boundary conditions, LINCS constraints for bond restrictions, Particle Mesh Ewald (PME) for long-range electrostatics, and a 1.2 nm cutoff for short-range interactions [51].

Molecular dynamics simulations were performed as single independent runs ($n = 1$) for each system. Specifically, separate 100 ns simulations were conducted for each unbound protein (PIK3CD, GNAI1, and GNAI3) and for each corresponding protein–ligand complex (PIK3CD-bemadienolide, GNAI1-quercetin, and GNAI3-kaempferol), resulting in a total of six MD simulation systems. Trajectory analyses included root-mean-square deviation (RMSD), root-mean-square fluctuation (RMSF), radius of gyration (Rg), and hydrogen bond formation to evaluate the structural stability and flexibility of the protein–ligand complexes [52].

2.7 Non-bonded interaction energy calculation

Average non-bonded interaction energies were calculated to quantify the strength and stability of phytoconstituent-protein interactions during the 100 ns molecular dynamics simulations. The total interaction energy (E_{int}) was determined as the sum of the short-range Lennard-Jones and Coulombic interaction energies according to:

$$E_{int} = E_{LJ} + E_{Coul}$$

where $E_{int}$is the total average non-bonded interaction energy (kcal/mol), E_{LJ} represents the short-range Lennard-Jones interaction energy, and E_{Coul} denotes the short-range Coulombic interaction energy. The average values of $E_{LJ}$and E_{Coul}were extracted from the trajectory energy files using the gmx energy module in GROMACS. More negative values of E_{int} indicate stronger and more

favorable protein-ligand interactions, reflecting enhanced hydrophobic and electrostatic.

2.8 MM-PBSA binding free energy calculations

The binding energies (ΔG_bind) of the protein-ligand complexes were estimated using the MM-PBSA approach in gmx_MMPBSA (v1.4.3) and AMBER MMPBSA.py. MD trajectory snapshots from 50 to 85 ns were analyzed to quantify contributions from van der Waals forces, electrostatic interactions, polar solvation, and non-polar solvation. This time window was selected based on RMSD equilibration and convergence of structural fluctuations, ensuring that only thermodynamically stable and well-equilibrated conformations were included in the binding free energy estimation, thereby improving the reliability and statistical robustness of the results. The MM-PBSA calculations were used to decompose the binding free energy into van der Waals, electrostatic, polar solvation, and non-polar solvation energy components. The overall binding free energy was expressed as:

$$\Delta G_{bind} = \Delta H - T\Delta S$$

where ΔH represents the enthalpic contribution derived from molecular mechanics and solvation terms, while TΔS represents the entropic contribution estimated using normal mode analysis. Due to the high computational cost of entropy calculations, normal mode analysis was performed on a representative subset of snapshots extracted from the equilibrated trajectory region, consistent with previously reported protocols [53].

Convergence of ΔG_bind was further assessed by monitoring energy stability across the selected trajectory interval, confirming consistent binding energy behavior. The binding free energy was decomposed into van der Waals, electrostatic, polar solvation, and non-polar solvation contributions. Entropy contributions (TΔS) were estimated using normal mode analysis performed on a representative subset of snapshots extracted from the equilibrated trajectory due to the high computational cost of full-frame entropy calculations [54].

2.9 Principal component analysis (PCA)

Principal component analysis (PCA) was performed to identify the dominant collective motions of the protein during molecular dynamics simulations in both unbound (apo) and ligand-bound systems, following established molecular dynamics protocols [52]. The covariance matrix of Cα atomic positional fluctuations was computed using the gmx_mpi covar module in GROMACS, and the corresponding eigenvectors and eigenvalues were extracted. In this analysis, eigenvectors represent the directions of collective atomic motions, whereas eigenvalues indicate the magnitude of variance associated with each principal component.

The percentage variance explained by the first and second principal components was calculated from the eigenvalues obtained from the eigenvalue.xvg file according to:

$$\text{PC1 variance (\%)} = \frac{\lambda_1}{\sum_{i=1}^{5}\lambda_i} \times 100$$

$$\text{PC2 variance (\%)} = \frac{\lambda_2}{\sum_{i=1}^{5}\lambda_i} \times 100$$

where λ_1 and λ_2 represent the first and second eigenvalues, respectively, and $\sum_{i=1}^{5}\lambda_i$ denotes the sum of the first five eigenvalues. The cumulative variance explained by PC1 and PC2 was calculated as:

$$\text{Cumulative variance (\%)} = \text{PC1 variance (\%)} + \text{PC2 variance (\%)}$$

A cumulative variance of ≥ 50% was considered indicative that the first two principal components captured the majority of the protein's essential conformational motions and, therefore, adequately represented the dominant dynamics of the system [53].

2.10 Pharmacokinetic and toxicity (ADMET) prediction

Canonical SMILES of top-ranked phytochemicals were analyzed in SwissADME (http://www.swissadme.ch/) to evaluate their pharmacokinetics properties and drug-likeness, while potential toxic effects were done in ProTox-II (https://tox-new.charite.de/protox_II/), predicting hepatotoxicity, mutagenicity, and acute toxicity. ADMET profiles guided selection of compounds for further drug development studies [55].

3 Results

3.1 Phytochemical retrieval and screening

A total of 242 *Warburgia ugandensis* phytochemicals were retrieved from literature sources and the COCONUT database. After standardization, duplicate removal, and canonicalization, 89 unique compounds were obtained. Subsequent stringent filtering steps resulted in 21 compounds being retained for further analysis (Fig. 2). The molecular properties of these 21 compounds satisfied drug-likeness and oral bioavailability criteria, as presented in Table 1, indicating favorable pharmacokinetic potential.

3.2 Target gene prediction and overlap with colorectal cancer

SwissTargetPrediction identified 435 potential targets for the 21 phytochemicals. Colorectal cancer–associated genes retrieved from GeneCards totaled 20,094

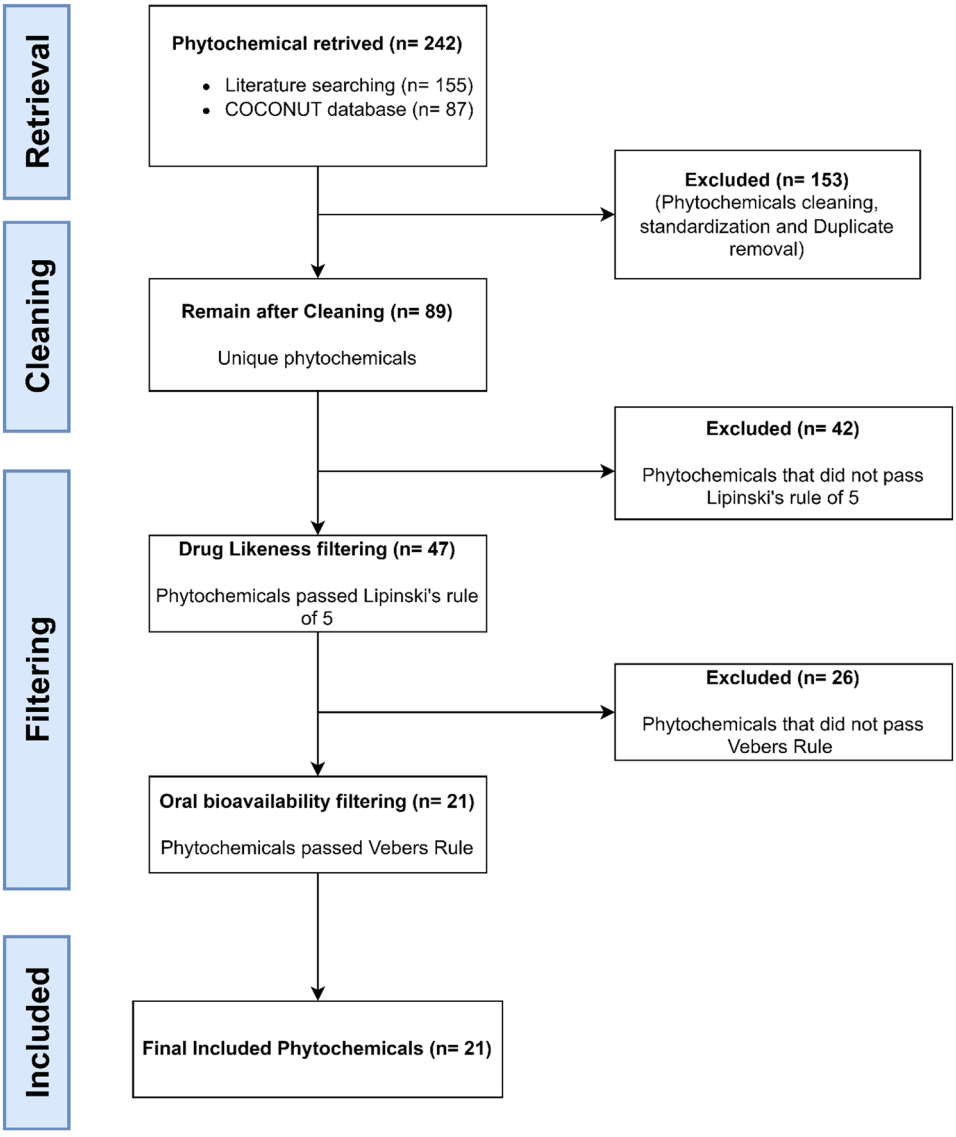

Fig. 2 Phytochemical retrieval and screening workflow for *Warburgia ugandensis* compounds, from initial retrieval and data cleaning to filtering and final selection of phytochemicals

protein-coding genes. Intersection analysis revealed 411 common targets, representing potential therapeutic targets of *W. ugandensis* phytochemicals in colorectal cancer (Fig. 3A).

3.3 Protein-protein interaction (PPI) network and hub gene identification

The 411 overlapping genes used to construct a protein to protein interaction (PPI) network in STRING, resulting in 460 nodes and 527 high-confidence interactions (score ≥ 0.9) (Fig. 3B). Subsequent analysis in Cytoscape using the CytoHubba MCC algorithm identified the top ten hub genes including: PIK3CA, PIK3R1, PIK3CB, PIK3CD, PIK3R2, PIK3R3, SRC, GNAI1, GNAI2, and GNAI3 (Fig. 3C). These hub genes are predominantly components of the PI3K signaling pathway and G protein-coupled signaling, highlighting their central roles in colorectal cancer-associated molecular networks.

3.4 Functional enrichment analysis

Functional annotation of the hub genes using GO revealed significant enrichment in key biological processes, including phosphatidylinositol phosphate biosynthesis, insulin receptor signaling, and PI3K signaling (Fig. 4A). Cellular component analysis indicated localization to the extrinsic membrane and PI3K complex (Fig. 4B), while molecular function enrichment highlighted phosphoinositide kinase activities (Fig. 4C). KEGG pathway analysis identified regulation of lipolysis in adipocytes, platelet activation, and relaxin signaling

Table 1 Molecular properties of selected *Warburgia ugandensis* phytochemicals

Compound_Name	MW	LogP	HBD	HBA	MR	TPSA	RB
Warburganal	250.338	2.278	1	3	69.0068	54.37	2
Ugandensidial	308.374	1.8196	1	5	79.9438	80.67	3
Mukaadial	266.337	1.2488	2	4	70.3966	74.6	2
Muzigadial	248.322	2.054	1	3	68.9128	54.37	2
Ugandenial A	266.337	1.7554	2	4	68.9776	66.76	0
Dendocarbin A	250.338	2.6405	1	3	67.5178	46.53	0
Dendocarbin L	266.337	1.7554	2	4	68.9776	66.76	0
Cinnamodial	308.374	1.8196	1	5	79.9438	80.67	3
Drimenin	234.339	3.3221	0	2	66.378	26.3	0
Drimendiol	238.371	2.7499	2	2	69.5906	40.46	2
Bemadienolide	232.323	3.2422	0	2	66.354	26.3	0
Ugandensolide	308.374	1.9786	1	5	78.7748	72.83	1
Pereniporin A	268.353	1.1996	3	4	70.2274	69.92	0
Isodrimeninol	236.355	3.1139	1	2	67.3778	29.46	0
Pereniporin B	266.337	1.4078	2	4	69.2276	66.76	0
Kaempferol	286.239	2.2824	4	6	74.5792	111.13	1
Quercetin	302.238	1.988	5	7	76.244	131.36	1
Cinnamolide	234.339	3.3221	0	2	66.378	26.3	0
Drimenol	222.372	3.7775	1	1	68.1788	20.23	1
futronolide	250.338	2.437	1	3	67.8378	46.53	0
Canellal	248.322	2.054	1	3	68.9128	54.37	2
*5-Fluorouracil (5-FU)	130.08	-0.9	2	3	26.5	58.2	0

MW = molecular mass(Da), LogP = lipophilicity, HBD = hydrogen bond donors, HBA = hydrogen bond acceptors, MR = molar refractivity, TPSA = topological polar surface area (Å^2), RB = rotatable bonds.* represent reference compounds (Positive control)

as significant pathways (Fig. 4D). Additionally, chemical carcinogenesis-receptor activation was among the notable pathways (Fig. 4E).

3.5 Molecular docking results

Docking of 21 phytochemicals against the 10 hub proteins revealed strong binding for flavonoids (Quercetin, Kaempferol) and drimane-type sesquiterpenes (Dendocarbin A, Dendocarbin L, Bemadienolide, Drimenin, Futronolide). For GNAI1, top binders included Quercetin (−9.8 kcal/mol), Kaempferol (−9.2 kcal/mol), and Dendocarbin A (−8.8 kcal/mol). GNAI3 binding was strongest for Quercetin (−9.6 kcal/mol), Kaempferol (−9.1 kcal/mol), and Dendocarbin A (−8.4 kcal/mol). PIK3CA exhibited highest affinities with Dendocarbin L (−8.6 kcal/mol), Dendocarbin A (−8.5 kcal/mol), and Bemadienolide (−8.2 kcal/mol). Other proteins showed moderate interactions (Table 2). For comparison, the reference compound 5-Fluorouracil exhibited consistently weaker binding across all targets, with docking scores ranging from approximately − 4.5 to − 5.3 kcal/mol, indicating substantially lower binding affinity relative to the screened phytochemicals. The distribution of binding affinities indicated that GNAI1, GNAI3, and PIK3CA were most strongly bound by these compounds (Figs. 5 and 6).

Analysis of protein-ligand interactions for the top-rated compounds revealed diverse binding modes. Quercetin-GNAI1 formed hydrogen bonds, π-cation, π-anion, and π-alkyl interactions, particularly involving residues Thr181, Val179, Arg178, Ala326, Glu43, Lys273, Asp150, and Asn259. Dendocarbin L-PIK3CA exhibited hydrogen bonds, π-sigma, and van der Waals interactions with residues Cys838, Gly837, Leu755, Phe666, Leu632, Gln630, Ser629, and His673. Kaempferol-GNAI3 engaged in π-sigma, π-alkyl, π-anion, π-cation, and hydrogen bonds with residues Asp272, Ala326, Lys270, Thr327, Asn269, Asp150, Leu273, and Cys325, among others. Bemadienolide-PIK3CD formed hydrogen bonds, π-sigma, and van der Waals interactions involving residues Phe609, Gly814, Gln795, Met788, Gln792, Gln60, Leu613, and Leu612, among others (Fig. 7).

3.6 Molecular dynamics simulation analysis

3.6.1 RMSD, RMSF, radius of gyration (Rg), hydrogen bonds

Molecular dynamics (MD) simulations of *Warburgia ugandensis* phytoconstituents; bemadienolide, quercetin, and kaempferol bound to colorectal cancer targets PIK3CD, GNAI1, and GNAI3 were performed for 100 ns to evaluate complex kinetic stability and interaction dynamics. Analyses included RMSD, RMSF, Rg, hydrogen bond formation, and non-bonded interaction energies (Fig. 8). RMSD profiles indicated that all complexes equilibrated around 20 ns and remained stable, with unbound proteins showing RMSD values of 0.22–0.25 nm and ligand-bound complexes maintaining

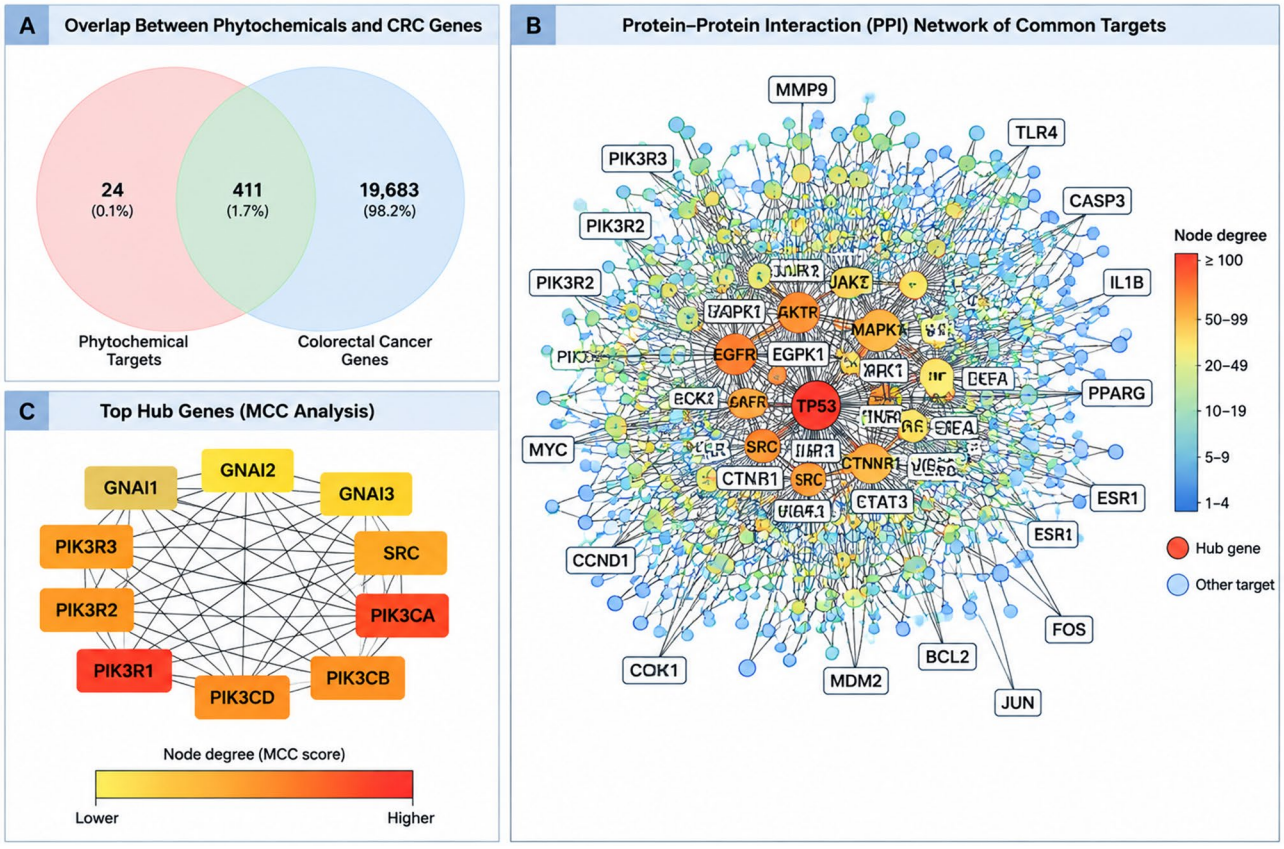

Fig. 3 Predicted molecular targets of *Warburgia ugandensis* phytochemicals and their relevance to colorectal cancer. (**A**) Venn diagram illustrating the intersection between phytochemical targets and CRC-associated genes. (**B**) Protein-protein interaction (PPI) network of the shared target genes. (**C**) The ten most highly connected hub genes identified using the CytoHubba plugin with the MCC algorithm

RMSD below 1.5 nm; GNAI1-Quercetin and GNAI3-Kaempferol displayed slightly lower fluctuations than PIK3CD-Bemadienolide. RMSF analysis showed reduced residue flexibility upon ligand binding, with Quercetin-GNAI1 (0.11 ± 0.07 nm) exhibiting the lowest fluctuations, followed by GNAI3-Kaempferol (0.13 ± 0.09 nm) and PIK3CD-Bemadienolide (0.15 ± 0.08 nm). Rg values ranged from 1.75 to 2.1 nm, indicating compact protein structures (Pawar et al., 2024), while hydrogen bond analysis revealed that Quercetin-GNAI1 maintained 3–4 stable bonds, GNAI3-Kaempferol formed 2–3 bonds, and PIK3CD-Bemadienolide had up to 2 bonds with occasional transient breakage.

3.6.2 Non-bonded interaction energies

Non-bonded interaction energies (Table 3) revealed that PIK3CD-Bemadienolide exhibited the strongest overall interactions (− 161.2 ± 17.2 kcal·mol^{-1}), primarily driven by van der Waals forces (− 122.6 ± 8.5 kcal·mol^{-1}). Similarly, GNAI3-Kaempferol (− 143.9 ± 43.1 kcal·mol^{-1}) and Quercetin-GNAI1 (− 124.6 ± 38.7 kcal·mol^{-1}) displayed substantial hydrophobic stabilization, with electrostatic contributions serving as secondary but significant components.

3.6.3 MM-PBSA evaluation of protein-ligand binding energies

MM-PBSA analysis over 50–85 ns (Table 4) estimated total binding free energies (ΔG_TOTAL) of − 86.2 ± 3.3 kcal·mol^{-1} for Quercetin-GNAI1, − 80.0 ± 3.1 kcal·mol^{-1} for GNAI3-Kaempferol, and − 71.0 ± 2.9 kcal·mol^{-1} for PIK3CD-Bemadienolide. The strong binding of Quercetin-GNAI1 was primarily driven by van der Waals (− 38.5 ± 1.5 kcal·mol^{-1}) and electrostatic (− 2.3 ± 0.1 kcal·mol^{-1}) interactions. Gas-phase energy (ΔG_GAS) contributed most significantly to binding, whereas solvation energy (ΔG_SOLV) provided minor stabilizing effects. Overall, these results suggest that hydrophobic contacts, hydrogen bonding, and π–π stacking work together to stabilize the complexes, with Quercetin-GNAI1 displaying the most favorable dynamic and energetic profile. Convergence analysis of MM-PBSA calculations over the 50–85 ns interval showed stable ΔG_bind values with minimal fluctuations, indicating that the selected trajectory window represents a

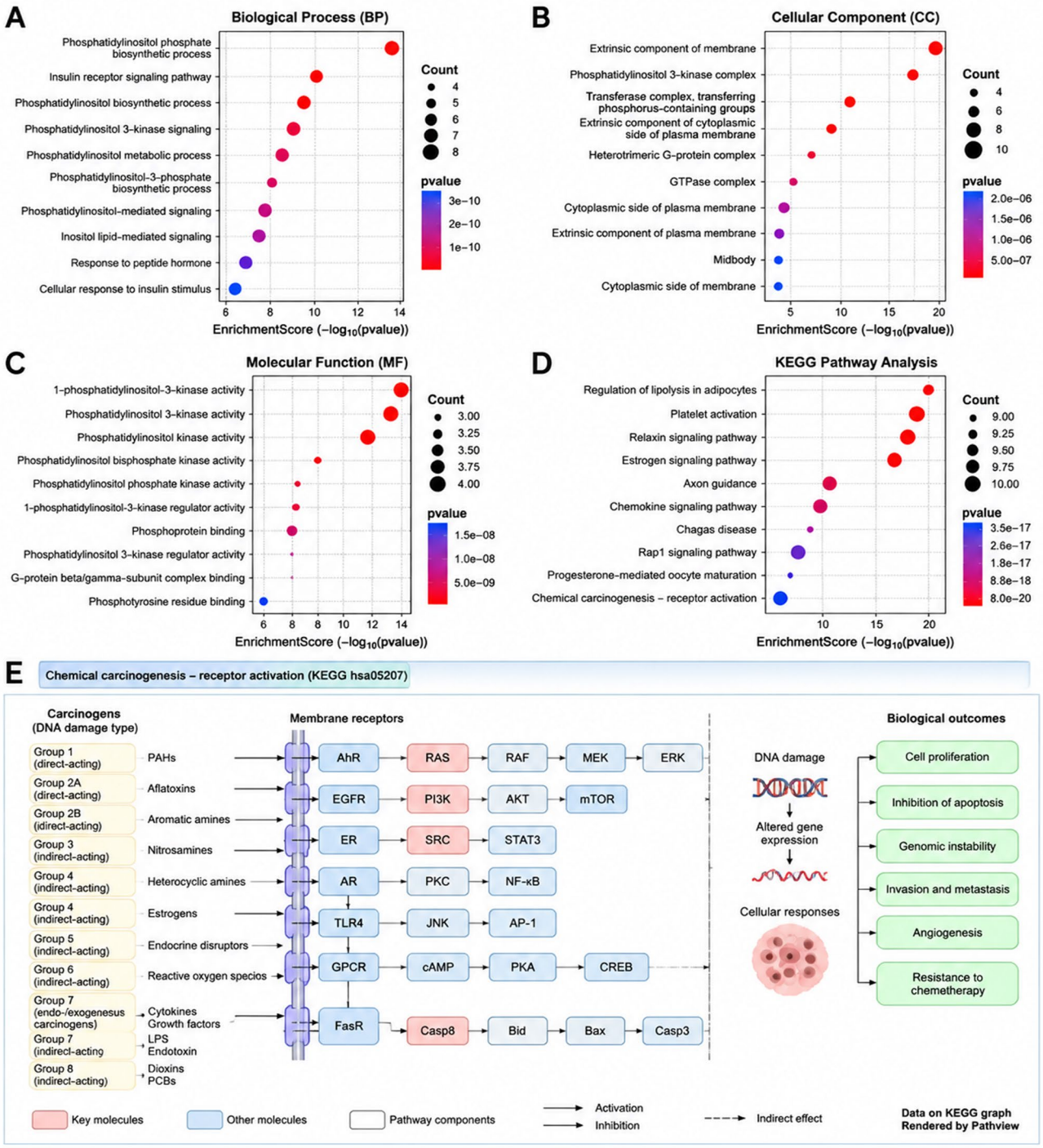

Fig. 4 Functional enrichment analysis of hub genes. (**A**-**C**) Gene Ontology (GO) enrichment depicting Biological Process (**A**), Cellular Component (**B**), and Molecular Function (**C**) categories. (**D**-**E**) KEGG pathway enrichment analysis showing overall significantly enriched pathways (**D**) and highlighting the Chemical Carcinogenesis-Receptor Activation pathway (**E**)

thermodynamically equilibrated state suitable for reliable binding free energy estimation.

3.6.4 Principal component analysis (PCA)

PCA of MD trajectories (Fig. 9) captured dominant motions along two principal components (PC1 and PC2). Unbound proteins showed broad, dispersed distributions, reflecting higher flexibility. Ligand-bound complexes exhibited tighter clusters, indicating restricted motion and increased structural rigidity. Quercetin-GNAI1 and GNAI3-Kaempferol displayed the most confined motion, whereas PIK3CD-Bemadienolide sampled

Table 2 Top 3 phytochemical ligands for each protein target with predicted binding affinities (kcal/mol)

Protein (PDB-ID)	Compound	Binding Affinity (kcal/mol)
GNAI1 (5JS7)	Quercetin*	−9.8
	Kaempferol	−9.2
	Dendocarbin A	−8.8
	5-Fluorouracil**	−4.6
GNAI3 (8OY1)	Quercetin*	−9.6
	Kaempferol	−9.1
	Dendocarbin A	−8.4
	5-Fluorouracil**	−4.8
PIK3CA (7R9V)	Dendocarbin L*	−8.6
	Dendocarbin A	−8.5
	Bemadienolide	−8.2
	5-Fluorouracil**	−5.2
GNAI2 (9K6L)	Kaempferol*	−6.4
	Quercetin	−6.3
	Dendocarbin A	−6.0
	5-Fluorouracil**	−4.5
PIK3CB (4BFR)	Isodrimeninol*	−8.2
	Quercetin	−8.1
	Dendocarbin A	−7.9
	5-Fluorouracil**	−5.0
PIK3CD (5DXU)	Bemadienolide*	−8.7
	Dendocarbin L	−8.1
	Kaempferol	−8.1
	5-Fluorouracil**	−5.1
PIK3R1 (3I5R)	Cinnamodial*	−6.9
	Dendocarbin L	−6.8
	Drimenol	−6.2
	5-Fluorouracil**	−4.9
PIK3R2 (2KT1)	Dendocarbin A*	−5.8
	Drimenin	−5.7
	Bemadienolide	−5.5
	5-Fluorouracil**	−4.7
PIK3R3 (5ZUT)	Quercetin*	−6.9
	Kaempferol	−6.5
	Dendocarbin L	−6.3
	5-Fluorouracil**	−4.6
SRC (8BQ3)	Quercetin*	−6.8
	Kaempferol	−6.5
	Dendocarbin A	−6.2
	5-Fluorouracil**	−5.3

*The top-rated compound for each protein target. **Reference compound (Positive control)

a wider conformational space, consistent with its higher kinetic flexibility observed in RMSD and RMSF.

As shown in Table 5, PC1 and PC2 jointly accounted for 41.9–70.0% of the variance captured within the retained eigenvectors across the six systems, with PIK3CD-Bemadienolide showing the largest cumulative contribution (69.99%) and GNAI3 the smallest (41.86%), consistent with the relative ordering of conformational flexibility described in the previous paragraph.

3.7 ADMET analysis

The ADME and toxicity profiles of the screened *Warburgia ugandensis* phytoconstituents; Quercetin, Kaempferol, Dendocarbin A, Dendocarbin L, Isodrimeninol, and Bemadienolide were evaluated. All compounds exhibited high GI absorption, while blood-brain barrier (BBB) permeability and P-glycoprotein substrate status (epithelial wall permeability) varied among ligands. Inhibition of cytochrome P450 enzymes (CYP1A2, CYP2C19, CYP2C9, CYP2D6, and CYP3A4) was observed selectively, suggesting potential for drug to drug interactions. Predicted Log Kp values (skin permeation) indicated moderate skin permeability (Table 6). Toxicity assessment showed no hepatotoxicity for most compounds, with variable carcinogenicity, immunotoxicity, mutagenicity, and cytotoxicity profiles. Predicted LD50 values ranged from 841 to 5000 mg/kg, and the compounds were classified between toxicity classes 3 to 5, indicating mostly low to moderate toxicity (Table 7).

4 Discussion

Colorectal cancer (CRC) continues to pose a significant global health challenge, as therapeutic options are often limited by drug resistance and associated adverse effects [56, 57]. Natural products are increasingly explored as alternative therapies due to their safety and multi-targeted actions [58, 59]. In present study, we applied an integrated in-silico approaches to predict the anti-CRC potential of compounds from *Warburgia ugandensis*, identify key protein targets, and explore possible molecular mechanisms. While these findings are predictive and have not been experimentally validated, they provide a prioritized list of candidate compounds and potential insights into their mechanism of action, which may guide future preclinical studies.

The identification of 21 drug-like phytochemicals from *W. ugandensis* highlights its chemical richness and therapeutic potential. Predominant among these were flavonoids, including quercetin and kaempferol, and drimane-type sesquiterpenes, such as dendocarbin A, dendocarbin L, bemadienolide, and warburganal, with several novel sesquiterpenes expanding the species' known repertoire. Both classes have been proven to exhibit anticancer activities, including induction of programmed cell death, inhibition of proliferation, and modulation of inflammatory responses in colon cancer models [60–62]. Their coexistence suggests potential synergistic effects on interconnected pathways, characteristic of polypharmacological natural therapeutics [29, 63]. Favorable physicochemical properties, including molecular weight, hydrogen bonding potential, and lipophilicity, indicate good oral bioavailability, while drimane-type sesquiterpenes provide scaffolds for further anticancer agent development. These observations are

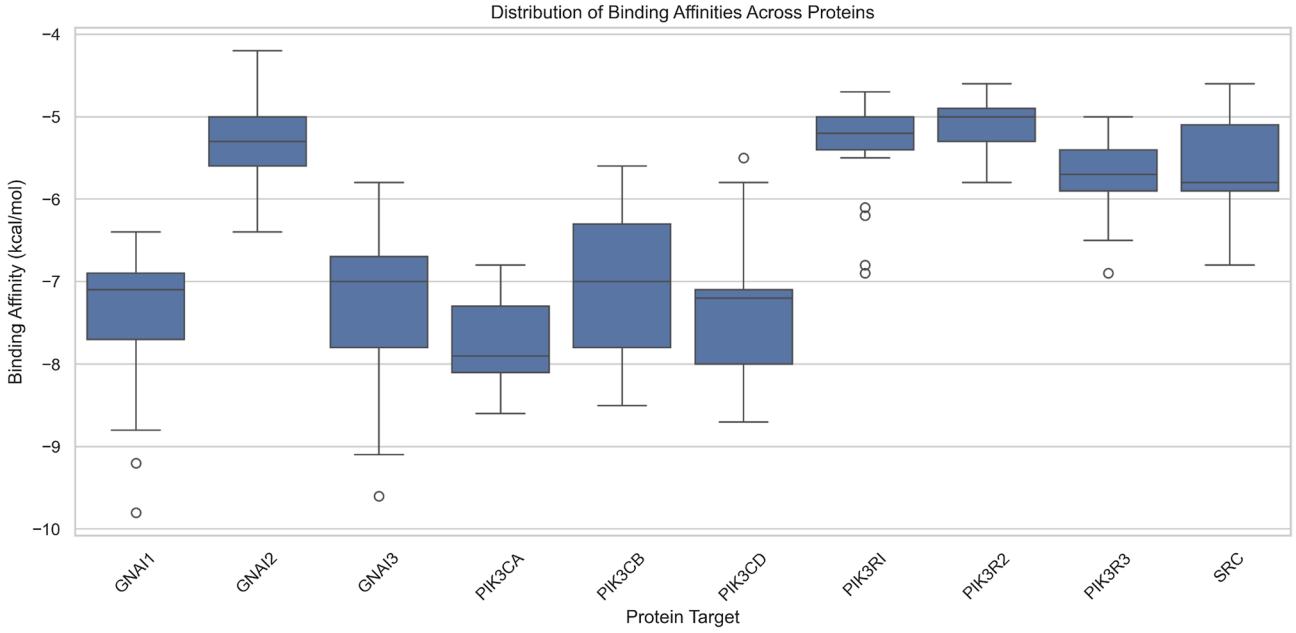

Fig. 5 Distribution of binding affinities across protein targets, highlighting strongest interactions

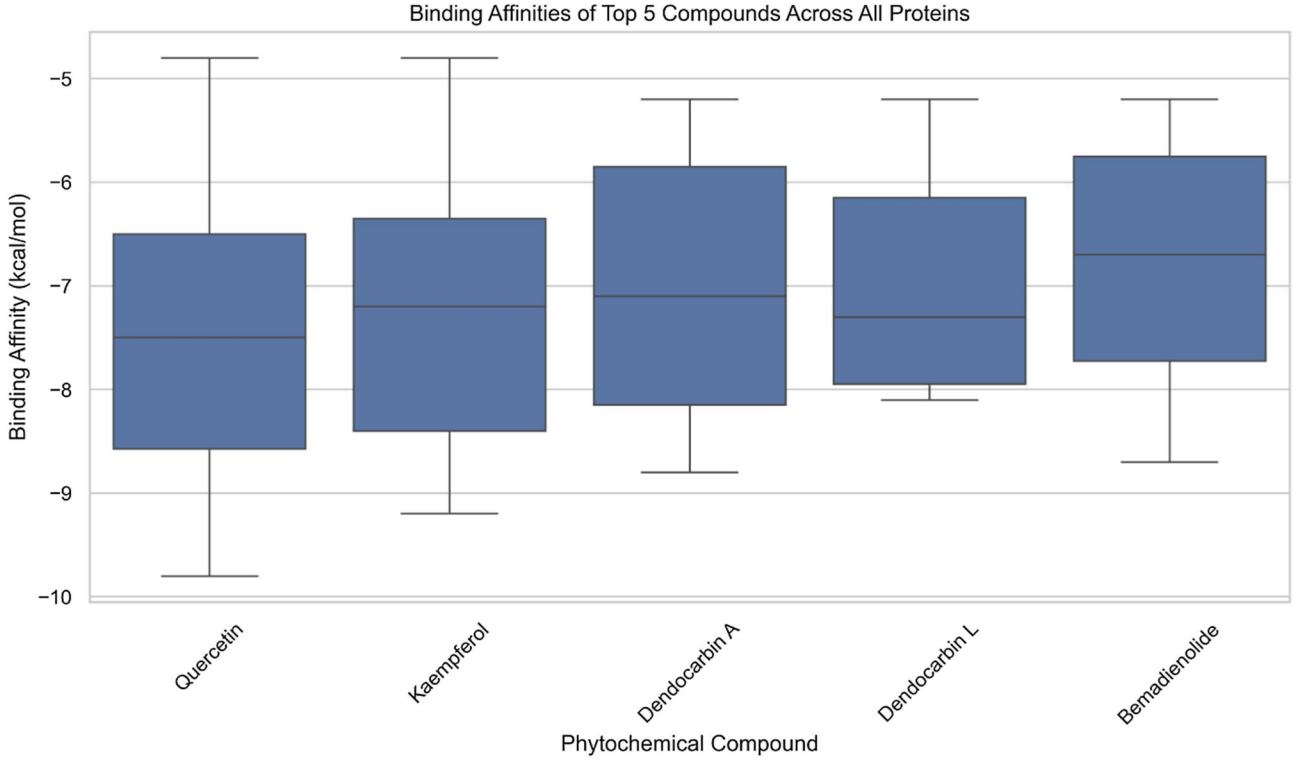

Fig. 6 Binding affinity distribution of the top five compounds across all proteins

consistent with previous reports showing that quercetin and kaempferol suppress CRC cell proliferation through apoptosis induction and PI3K/AKT pathway inhibition [64–67].

Network pharmacology analysis offered a system-level view of how *W. ugandensis* phytochemicals interact with CRC-related targets [68, 69]. A high number of overlapping targets with CRC-associated genes highlights a polypharmacological mode of action, typical of many plant-derived therapeutics [70–74]. Hub genes identified, including PIK3CA, SRC, and members of the GNAI family, are central regulators of proliferation, survival,

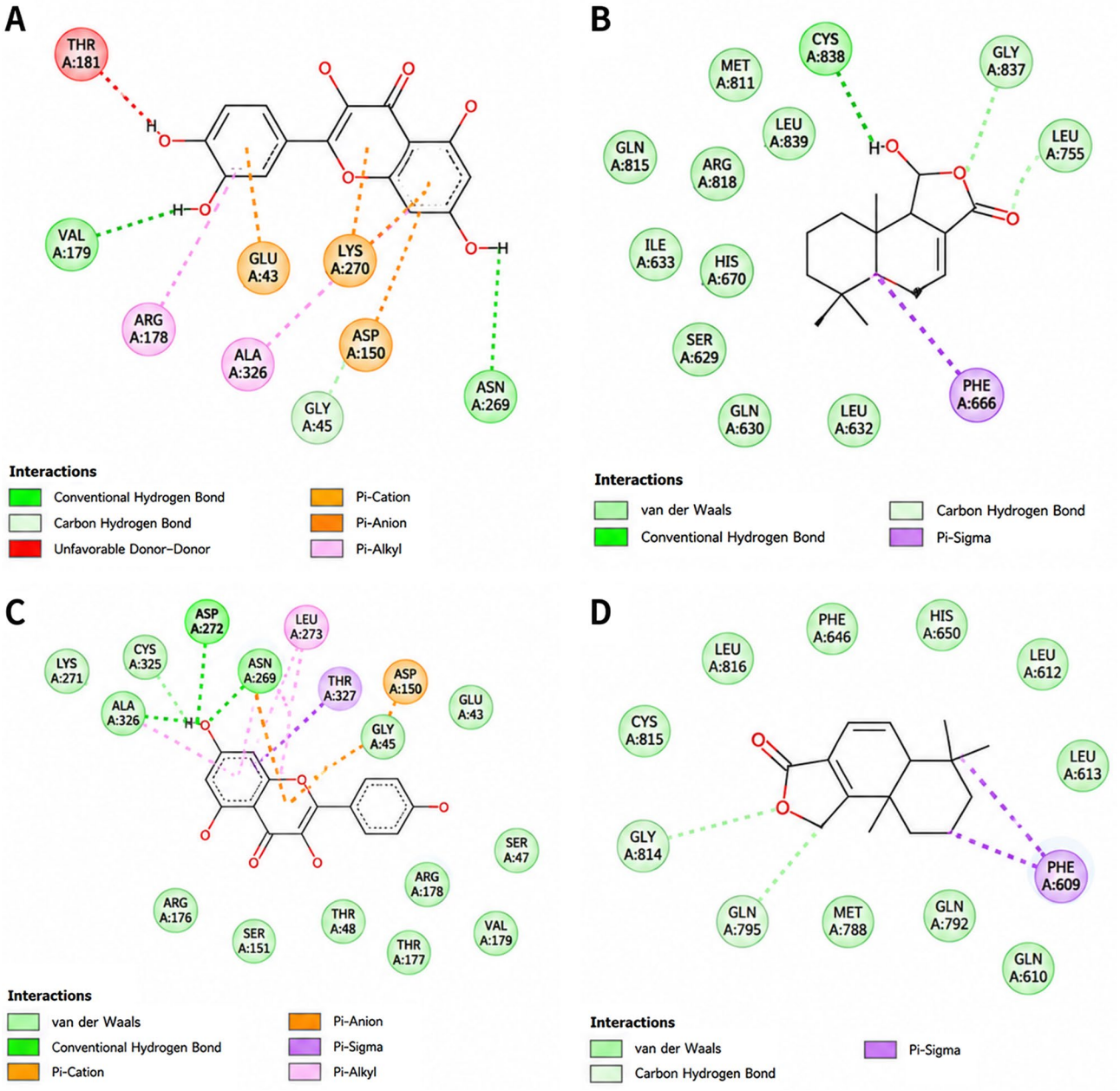

Fig. 7 2D interaction diagrams of top-rated phytochemicals with respective protein targets: (**A**) Quercetin-GNAI1, (**B**) Dendocarbin L-PIK3CA, (**C**) Kaempferol-GNAI3, (**D**) Bemadienolide-PIK3CD

and metastatic signaling in CRC [75, 76]. This suggests that *W. ugandensis* compounds could simultaneously modulate multiple oncogenic drivers, consistent with the understanding that effective CRC interventions often require targeting interconnected signaling networks rather than single proteins, which may lead to therapy resistance [77]. The prominence of PI3K and G-protein-related hubs provides a mechanistic explanation for the observed antiproliferative and pro-apoptotic effects of *W. ugandensis* metabolites, aligning with studies showing flavonoids and sesquiterpenes interfere with these pathways [78]. Similar network pharmacology studies on medicinal plants have also identified PIK3CA, SRC, and GNAI family genes as central CRC regulatory hubs, further supporting their critical role in tumor progression and therapeutic targeting [79–81].

Gene Ontology (GO) and KEGG pathway enrichment analyses further supported these findings by highlighting biological processes and signaling pathways that are critical to CRC progression [82]. Enriched pathways included phosphoinositide kinase activity, insulin receptor signaling, and PI3K-Akt signaling, all of which play

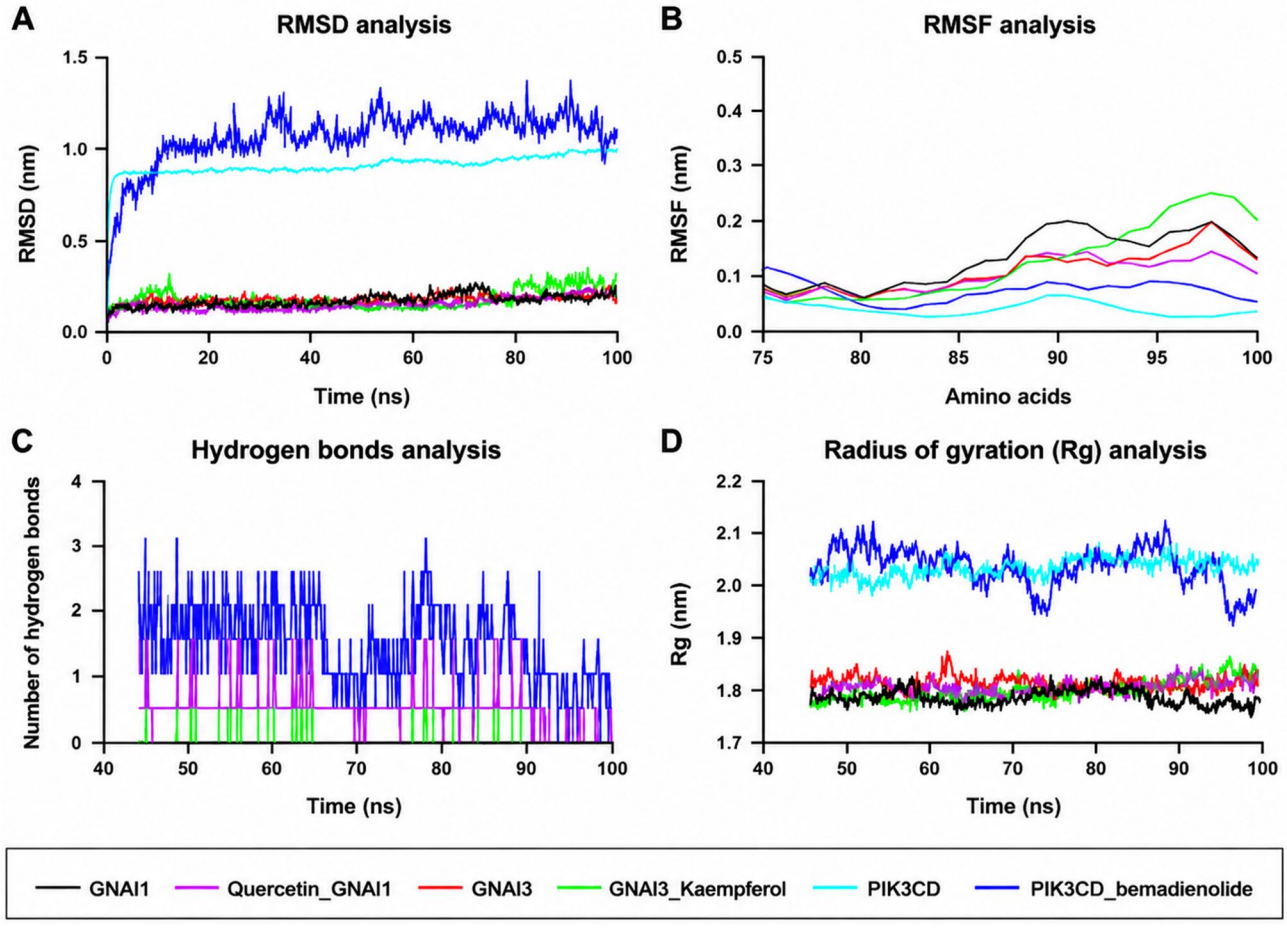

Fig. 8 Molecular dynamics analysis of *Warburgia ugandensis* phytoconstituents (bemadienolide, quercetin, and kaempferol) bound to colorectal cancer targets (PIK3CD, GNAI1, and GNAI3) over 100 ns. Plots show RMSD, RMSF, Rg, and hydrogen bond formation, highlighting complex stability and dynamic behavior

Table 3 Non-bonded interaction energies of the protein-ligand complex at the stable region, 50-85ns

Complex	Coulomb (kcal/mol)	Lennard-Jones (kcal/mol)	Sum of Coulomb and Lennard-Jones (kcal/mol)
PIK3CD-bemadienolide	-38.6 ± 8.7	-122.6 ± 8.5	-161.2 ± 17.2
GNAI3-Kaempferol	-48.0 ± 23.5	-95.9 ± 19.6	-143.9 ± 43.1
Quercetin-GNAI1	-40.1 ± 21.1	-84.5 ± 17.6	-124.6 ± 38.7

central roles in tumor growth, proliferation, and survival [83]. GO analysis additionally revealed enrichment of phosphatidylinositol metabolic processes, phosphatidylinositol 3-kinase signaling, and cellular responses to insulin stimulation, suggesting that modulation of the PI3K/AKT signaling axis may represent a key mechanism underlying the therapeutic effects of *W. ugandensis* phytochemicals [30]. These findings are particularly relevant to CRC pathogenesis because phosphoinositides act as critical lipid second messengers that regulate cell proliferation, migration, survival, and metabolism through downstream effectors, including AKT and mTOR [84, 85]. Dysregulation of this signaling network, frequently driven by mutations in genes such as PIK3CA, PTEN, and KRAS, contributes substantially to CRC initiation and progression [86, 87].

KEGG pathway analysis also identified enrichment of platelet activation, relaxin signaling, and regulation of lipolysis in adipocytes, pathways that are not traditionally regarded as canonical CRC pathways. Nevertheless, these pathways may reflect broader tumor-promoting mechanisms that converge on major oncogenic networks, particularly PI3K/AKT and MAPK signaling. Platelet activation is increasingly recognized as an important contributor to CRC progression because activated platelets protect circulating tumor cells from immune surveillance, promote epithelial-mesenchymal transition, and facilitate metastatic colonization [88, 89]. Similarly, relaxin signaling has been implicated in

Table 4 MMPBSA analysis of the complex systems at the stable region, 50-85ns

Characteristics	PIK3CD- Bemadienolide (kcal/mol)	Quercetin-GNAI1 (kcal/mol)	GNAI3-Kaempferol (kcal/mol)
ΔVDWAALS	-32.11 ± 1.3	-38.5 ± 1.5	-35.8 ± 1.4
ΔEEL	-1.21 ± 0.1	-2.3 ± 0.1	-1.9 ± 0.1
ΔEGB	1.88 ± 0.0	2.1 ± 0.1	1.9 ± 0.1
ΔESURF	-4.08 ± 0.0	-4.4 ± 0.1	-4.2 ± 0.1
ΔGGAS	-33.32 ± 1.5	-40.8 ± 1.6	-37.7 ± 1.5
ΔGSOLV	-2.20 ± 0.0	-2.3 ± 0.1	-2.3 ± 0.1
ΔTOTAL	-71.04 ± 2.9	−86.2 ± 3.3	−80.0 ± 3.1

ΔVDWAALS denotes the van der Waals interaction energy, whereas ΔEEL represents the electrostatic interaction component. ΔEGB corresponds to the polar contribution to solvation energy calculated using the GB/PB approach, while ΔESURF reflects the non-polar solvation component derived from the solvent-accessible surface area. The gas-phase energy (ΔGGAS) is obtained as the sum of ΔVDWAALS and ΔEEL, whereas the total solvation energy (ΔGSOLV) combines ΔEGB and ΔESURF. Finally, ΔTOTAL represents the overall binding stability of each protein-ligand complex

Table 5 Percentage variance calculated from the PC1 and PC2 for each simulated system, expressed relative to the retained eigenvectors

System	λ1 (PC1), nm^2	λ2 (PC2), nm^2	PC1 (%)	PC2 (%)	Cumulative PC1 + PC2 (%)
GNAI1 (unbound)	0.5644	0.2890	33.08	16.94	50.02
GNAI1-Quercetin (bound)	0.3691	0.2386	27.65	17.87	45.52
GNAI3 (unbound)	0.3606	0.2170	26.13	15.73	41.86
GNAI3-Kaempferol (bound)	0.6161	0.2006	39.07	12.72	51.79
PIK3CD (unbound)	8.7178	2.8247	46.46	15.05	61.51
PIK3CD-Bemadienolide (bound)	11.4055	3.5240	53.47	16.52	69.99

Percentages are expressed relative to the cumulative variance of the retained eigenvectors from each gmx covar calculation, not the total variance of the full conformational space

angiogenesis, extracellular matrix remodeling, and cell migration through activation of PI3K/AKT and MAPK

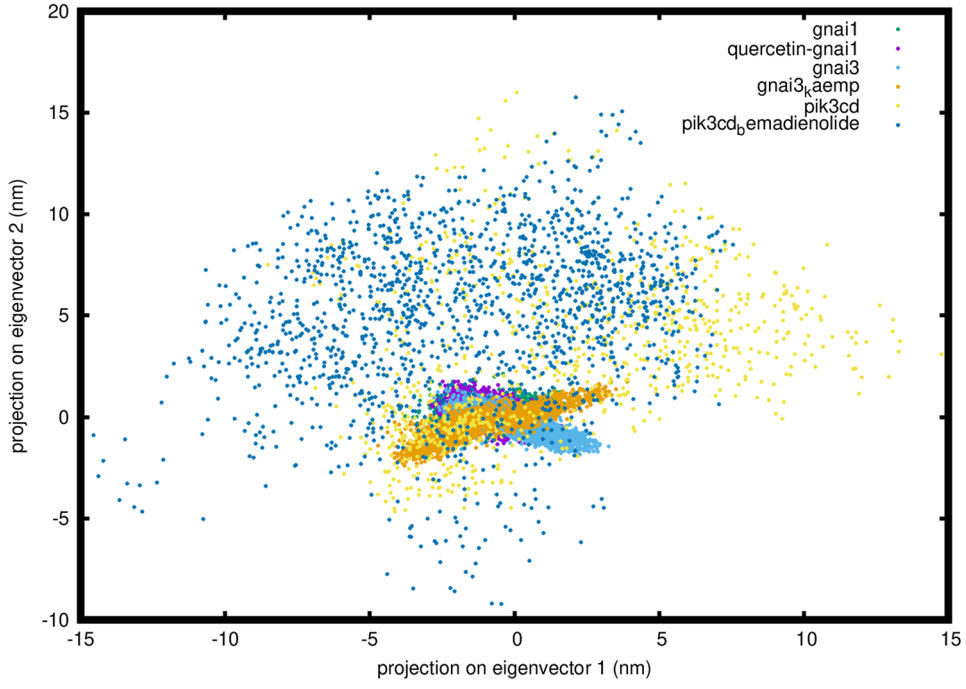

Fig. 9 PCA analysis of unbound GNAI1, GNAI3 and PIK3CD and their respective bound compounds (Quercetin, Kaempferol and bema), over 50 ns

Table 6 Pharmacokinetic properties of selected *Warburgia ugandensis* phytochemicals

Ligands	GI abs	BBB Perm	*P*-gp sub	CYP1A2 inhibitor*	CYP2C19 inhibitor*	CYP2C9 inhibitor*	CYP2D6 inhibitor*	CYP3A4 inhibitor*	Log Kp (cm/s)
C1	High	-	-	+	-	-	+	+	-7.05
C2	High	-	-	+	-	-	+	+	-6.70
C3	High	+	-	-	-	+	-	-	-5.35
C4	High	+	+	-	-	-	-	-	-6.54
C5	High	+	-	-	-	-	-	-	-5.53
C6	High	+	-	-	+	+	-	-	-5.18

Note: C1 = Quercetin; C2 = Kaempferol; C3 = Dendocarbin A; C4 = Dendocarbin L; C5 = Isodrimeninol; C6 = Bemadienolide; BBB, blood-brain barrier; GI, gastrointestinal

Table 7 Predicted toxicity properties of selected *Warburgia ugandensis* phytochemicals

Ligand	HpT	CaG	ImT	MuG	CyT	Toxicity Class	PrA (%)	LD50 (mg/kg)
Quercetin	-	+	-	+	-	3	100	159
Kaempferol	-	-	-	-	-	5	70.97	3919
Dendocarbin A	-	-	+	-	-	5	69.26	5000
Dendocarbin L	-	+	-	-	-	4	69.26	2000
Isodrimeninol	-	-	+	-	-	5	68.07	5000
Bemadienolide	-	-	-	-	-	4	68.07	841

Reference compounds. Active are indicated by "+", inactive by "–". HpT: Hepatotoxicity, CaG: Carcinogenicity, ImT: Immunotoxicity, MuG: Mutagenicity, CyT: Cytotoxicity, PrA: Prediction Accuracy. Toxicity classes: 1–2 = fatal, 3 = toxic, 4 = harmful, 5 = may be harmful, 6 = non-toxic

pathways [90–93]. These findings suggest that *W. ugandensis* may target not only primary tumor growth but also metastatic dissemination, which remains a major clinical challenge in CRC therapy.

Furthermore, the enrichment of pathways involved in the regulation of lipolysis in adipocytes may be biologically relevant because obesity, insulin resistance, and chronic inflammation are established risk factors for CRC that promote tumor growth through metabolic reprogramming and activation of pro-survival signaling pathways [94–96]. Collectively, these findings suggest that *W. ugandensis* phytochemicals may exert anti-CRC effects through the simultaneous modulation of interconnected pathways involved in tumor growth, metabolism, angiogenesis, and metastasis, supporting a potential multi-target mechanism of action. Nevertheless, because the enrichment analysis was based on a limited set of hub genes, the identified non-canonical pathways should be considered hypothesis-generating and require further validation using larger target datasets and experimental studies.

Molecular docking studies were used to characterize these interactions at the atomic level. Top-ranking compounds, including flavonoids (quercetin, kaempferol) and drimane-type sesquiterpenes (dendocarbin A, dendocarbin L, bemadienolide), exhibited strong binding to hub proteins such as PIK3CA, GNAI1, GNAI3, and SRC. These results align with known kinase-inhibitory effects of flavonoids and the potential of drimane sesquiterpenes as PI3K modulators [76, 97, 98]. Detailed binding analyses revealed stable non-covalent interactions with residues critical for enzyme activation, confirming the potential to interfere with oncogenic signaling cascades [99]. Observed binding modes are consistent with flavonoid inhibition of kinases and G-protein-coupled pathways [100, 101], while drimane-type sesquiterpenes emerge as novel modulators of CRC-relevant targets. Strong interactions with multiple hub proteins suggest potential synergistic or additive effects in-vivo, supporting the concept of multi-targeted therapeutics from a single plant source [102, 103]. These compounds have also demonstrated anticancer activity in other in-vitro studies, reinforcing their potential efficacy against CRC [104–107].

Molecular dynamics (MD) simulations were used to assess the kinetic stability and persistence of interactions between *W. ugandensis* phytochemicals and CRC targets. Low RMSD and RMSF values indicated minimal structural deviations and reduced residue flexibility, suggesting ligand binding stabilized protein backbones and restricted unnecessary motion [108]. Compact Rg profiles and consistent hydrogen bond occupancy further supported maintenance of tight ligand-protein interactions, indicating structural integrity and compatibility under dynamic physiological conditions [109].

Non-bonded interaction analysis revealed that van der Waals forces predominantly stabilized the complexes, complemented by electrostatic interactions. The stronger van der Waals contribution in the PIK3CD-bemadienolide complex reflects steric compatibility with PI3K's binding cavity, while flavonoid complexes exhibited balanced hydrophobic and polar interactions [110]. MM-PBSA binding free energy analysis produced results consistent with these observations, showing favorable total free energies primarily contributed by van der Waals and electrostatic contributions. The quercetin-GNAI1 complex exhibited the most favorable predicted binding free energy, suggesting high binding affinity and potential biological relevance [111]. The reliability of the MM-PBSA results is supported by convergence of binding free energy values within the equilibrated simulation window, indicating stable protein-ligand interactions [112]. The consistent energetic profiles further confirm that ligand binding is maintained in a thermodynamically stable state. The use of representative snapshots for entropy estimation provides a reasonable approximation of entropic effects while maintaining computational feasibility, in line with established MM-PBSA protocols [113, 114].

Principal component analysis (PCA) revealed restricted conformational motion and reduced dynamic sampling in ligand-bound systems compared to unbound proteins, indicating increased structural rigidity upon ligand binding [115]. Compact clustering in quercetin-GNAI1 and kaempferol-GNAI3 complexes reflects energy minimization and stable folding, while broader distributions

in the PIK3CD-bemadienolide system suggest slightly higher flexibility due to larger binding pocket rearrangements [116]. These PCA outcomes reinforce the dynamic stabilization inferred from MD simulations and energy analyses.

Pharmacokinetic and toxicity (ADMET) analyses indicated high gastrointestinal absorption, good oral bioavailability, and minimal efflux for most compounds [117, 118]. Limited blood-brain barrier penetration reduces potential neurotoxicity, while favorable polar surface area and bioavailability scores indicate good membrane permeability [119, 120]. Importantly, CYP450 analysis indicated that some compounds may inhibit CYP3A4, suggesting a potential risk of cytochrome P450-mediated drug-drug interactions, which may limit their concurrent use with standard chemotherapeutic agents and could be mitigated through structural modification [121]. Toxicity predictions indicate low acute toxicity and limited dermal absorption, consistent with in-vitro studies reporting minimal cytotoxicity [122]. Notably, compound-specific toxicity profiling (Table 6) reveals safety trade-offs, where quercetin shows potential mutagenic and carcinogenic alerts despite strong binding affinity, while bemadienolide exhibits moderate acute toxicity (LD_{50} = 841 mg/kg), highlighting the need to balance predicted efficacy with safety considerations during lead optimization. Therefore, while both quercetin and bemadienolide emerge as promising lead compounds from a target-binding perspective, their therapeutic advancement would require careful dose optimization, structural refinement, and rigorous experimental toxicity validation to ensure a balance between efficacy and safety.

Overall, the integrated computational approaches demonstrate the polypharmacological potential of *W. ugandensis*, showing its ability to modulate key oncogenic targets, including GNAI1, GNAI3, PIK3CA, and SRC within PI3K/AKT and G-protein signaling pathways. These findings position *W. ugandensis* as a potential source of novel, multi-target anticancer compounds. Limitations of this study include reliance on computational predictions, which require experimental validation, and the potential underrepresentation of CRC heterogeneity. Additionally, the predictive approach was not benchmarked against small molecules with known anti-CRC activity, which limits the ability to assess the accuracy of the models in reflecting real biological effects. Also, no probability cutoff was applied during target prediction, which may have introduced lower-confidence interactions and potential noise in the initial dataset. Despite these limitations, this study provides a robust, hypothesis-generating framework for developing *W. ugandensis*-derived compounds as natural, multitarget therapeutics for CRC. We acknowledge that Lipinski's Rule of Five and Veber's rules may have excluded potentially bioactive "beyond Rule of 5" natural compounds. Future studies should consider less restrictive screening approaches to capture a broader range of bioactive molecules.

5 Conclusions and future perspectives

This study provides computational evidence suggesting that *Warburgia ugandensis* contains phytochemicals with potential multi-target activity relevant to colorectal cancer (CRC) biology. Network pharmacology and molecular docking analyses indicate possible interactions with key oncogenic regulators, particularly components of the PI3K-related signaling axis and G-protein-associated networks. Among the identified compounds, drimane-type sesquiterpenes emerged as notable candidates based on predicted binding affinities and network connectivity.

These findings suggest a plausible mechanistic basis through which *W. ugandensis* phytochemicals may influence CRC-associated pathways. However, it is important to emphasize that all conclusions are derived from in-silico analyses and therefore remain predictive. The proposed multi-target effects and pathway-level interactions should be interpreted as hypotheses requiring further experimental validation rather than confirmed biological activities. Overall, this work highlights the value of integrative computational approaches in prioritizing bioactive natural compounds for further investigation. It also supports the potential of ethnopharmacologically derived metabolites as starting points for anticancer drug discovery, particularly within multi-target therapeutic frameworks.

Future studies should prioritize experimental validation, including: (i) in-vitro cytotoxicity and mechanistic assays to confirm modulation of the PI3K/AKT and G-protein signaling pathways; (ii) target engagement assays to verify direct compound-protein interactions; and (iii) in-vivo pharmacokinetic and efficacy studies using colorectal cancer (CRC) animal models. Furthermore, medicinal chemistry optimization of drimane-type sesquiterpenes should be pursued to enhance their potency, selectivity, and metabolic stability. The combinatorial use of *Warburgia ugandensis* phytochemicals with standard CRC therapies should also be explored to identify potential synergistic effects and overcome therapeutic resistance mechanisms. In addition, future target-specific investigations should incorporate appropriate positive control compounds to benchmark the efficacy of the prioritized *W. ugandensis* phytochemicals against established therapeutic agents for each molecular target.

Acknowledgements
The authors thank the National Institutes of Health (NIH) Office of Data Science Strategy (ODSS) for their immense support before and during the October 2025 Omics codeathon organized by the Institute for Genomic

Medicine Research in collaboration with the African Society for Bioinformatics and Computational Biology (ASBCB).

Author contributions
YA conceived the original idea. YA, BN, APO, AAL, MBF, and OMK developed the computational pipeline, performed the bioinformatic analyses, and drafted the manuscript. YA, MBF, AJ and AAL contributed to writing, reviewing, and editing the manuscript. DRM provided Computational resources, reviewing, and editing the manuscript. OIA supervised the project, provided guidance, and conducted the final editing and review. All authors read and approved the final manuscript.

Funding
None.

Data availability
The dataset analyzed in this study is publicly available at the project home page: (https:/github.com/omicscodeathon/anticrcwu/tree/main/data). All data, figures, and instructions necessary to reproduce the analyses are contained in the project's GitHub repository (https://github.com/omicscodeathon/anticrcwu).

Declarations

Studies involving research on animals
No animal studies are presented in this manuscript.

Studies involving research on humans
No human studies are presented in the manuscript.

Inclusion of identifiable data
No potentially identifiable images or data are presented in this study.

Human ethics approval and consent to participate
Not applicable.

Consent for publication
Not applicable.

Generative AI disclosure
The authors declare that no generative AI was used in the creation of this manuscript.

Competing interests
The authors declare no competing interests.

Author details
[1]Department of Global Health and Biomedical Sciences, Nelson Mandela African Institution of Science and Technology, Arusha, United Republic of Tanzania
[2]Department of Molecular Biology and Biotechnology, University of Dar es Salaam, Dar es Salaam, United Republic of Tanzania
[3]Infectious Diseases Research Collaboration (IDRC), Makerere University, Kampala, Uganda
[4]Department of Integrated Science, Obafemi Awolowo University, Osun State, Nigeria
[5]Department of Biochemistry, Adekunle Ajasin University, Ondo State, Nigeria
[6]Molecular Biology and Simulation Centre, Ado-Ekiti, Ekiti State, Nigeria
[7]Department of Biological Sciences, Redeemer's University, Ede, Nigeria
[8]Department of Biochemistry and Cell Biology, University of Abomey-Calavi, Calavi, Benin
[9]Department of Biotechnology, University of the Western Cape, Bellville, South Africa
[10]Department of Science, Technology and Innovation/TIA Nanotechnology Platform, University of the Western Cape, Bellville, South Africa
[11]Molecular Diagnostic Department, Kansas Department of Health and Environment, Topeka, Kansas, USA
[12]Institute for Genomic Medicine Research, West Hartford, CT, USA
[13]African Society for Bioinformatics and Computational Biology, Cape Town, South Africa

Received: 20 February 2026 / Accepted: 10 September 2026
Published online: 01 October 2026

References

1. Arnold M, Sierra MS, Laversanne M et al Global patterns and trends in colorectal cancer incidence and mortality. Epub ahead of print 1 April 2017. https://doi.org/10.1136/gutjnl-2015-310912
2. Duan B, Zhao Y, Bai J et al Colorectal cancer: an overview. In: *Gastrointestinal cancers [Internet]*. Exon Publications. Epub ahead of print 30 September 2022. https://doi.org/10.36255/exon-publications-gastrointestinal-cancers-colorectal-cancer
3. IARC Working Group on the Evaluation of Cancer-Preventive Interventions (2019) *Colorectal cancer screening*. Lyon (FR): International Agency for Research on Cancer. http://www.ncbi.nlm.nih.gov/books/NBK553200/ accessed 16 June 2026)
4. Sawicki T, Ruszkowska M, Danielewicz A et al (2021) A Review of Colorectal Cancer in Terms of Epidemiology, Risk Factors, Development, Symptoms and Diagnosis. Cancers 13:2025
5. Siegel RL, Miller KD, Fedewa SA et al (2017) Colorectal cancer statistics, 2017. CA Cancer J Clin 67:177–193
6. Ogbodo UC, Jawali A, King'ori PW, Nsedu EI, Awe OI (2026) Mendelian randomization studies of lipid traits and risk of colorectal cancer: a systematic review. Consider Med. https://doi.org/10.1136/conmed-2025-000028
7. Rawla P, Sunkara T, Barsouk A (2019) Epidemiology of colorectal cancer: incidence, mortality, survival, and risk factors. Gastroenterol Rev Gastroenterol 14:89–103
8. Chang H, Lei L, Zhou Y et al (2018) Dietary Flavonoids and the Risk of Colorectal Cancer: An Updated Meta-Analysis of Epidemiological Studies. Nutrients 10:950
9. Macharia JM, Mwangi RW, Szabó I et al (2023) Regulatory activities of *Warbugia ugandensis* ethanolic extracts on colorectal cancer-specific genome expression dose-dependently. Biomed Pharmacother 166:115325
10. Wan M, Wang Y, Zeng Z et al (2020) Colorectal cancer (CRC) as a multifactorial disease and its causal correlations with multiple signaling pathways. Biosci Rep 40:BSR20200265
11. Zhao H, Ming T, Tang S et al (2022) Wnt signaling in colorectal cancer: pathogenic role and therapeutic target. Mol Cancer 21:144
12. Melincovici CS, Mihu CM, Mărginean M et al (2016) The prognostic significance of p53, Bax, Bcl-2 and cyclin E protein overexpression in colon cancer - an immunohistochemical study using the tissue microarray technique. Romanian J Morphol Embryol Rev Roum Morphol Embryol 57:81–89
13. Pashirzad M, Khorasanian R, Fard MM et al (2021) The therapeutic potential of MAPK/ERK inhibitors in the treatment of colorectal cancer. Curr Cancer Drug Targets 21:932–43
14. Stefani C, Miricescu D, Stanescu-Spinu I-I et al (2021) Growth Factors, PI3K/AKT/mTOR and MAPK Signaling Pathways in Colorectal Cancer Pathogenesis: Where Are We Now? Int J Mol Sci 22:10260
15. Bahrami A, Khalaji A, Bahri Najafi M et al (2024) NF-κB pathway and angiogenesis: insights into colorectal cancer development and therapeutic targets. Eur J Med Res 29:610
16. Erkasap N, Özyurt R, Özkurt M et al (2016) The role of JAK/STAT signaling pathway and TNF-α crosstalk in human colorectal cancer. Gene Rep 3:1–4
17. Hu M, Zhou X, Wang Y et al (2020) Relaxin-FOLFOX-IL-12 triple combination therapy engages memory response and achieves long-term survival in colorectal cancer liver metastasis. J Control Release Off J Control Release Soc 319:213–221
18. Li X, Wu Y, Tian T (2022) TGF-β Signaling in Metastatic Colorectal Cancer (mCRC): From Underlying Mechanism to Potential Applications in Clinical Development. Int J Mol Sci 23:14436
19. Luo C, Zhang H (2017) The Role of Proinflammatory Pathways in the Pathogenesis of Colitis-Associated Colorectal Cancer. Mediators Inflamm 2017:5126048
20. Tyagi A, Sharma AK, Damodaran C (2020) A Review on Notch Signaling and Colorectal Cancer. Cells 9:1549
21. Novoa Díaz MB, Carriere P, Gentili C (2023) How the interplay among the tumor microenvironment and the gut microbiota influences the stemness of colorectal cancer cells. World J Stem Cells 15:281–301

22. Ogbodo UC, Enejoh OA, Okonkwo CH et al (2023) Computational identification of potential inhibitors targeting cdk1 in colorectal cancer. Front Chem 11:1264808
23. Xie Y-H, Chen Y-X, Fang J-Y (2020) Comprehensive review of targeted therapy for colorectal cancer. Signal Transduct Target Ther 5:22
24. Zhai Z, Yu X, Yang B et al (2017) Colorectal cancer heterogeneity and targeted therapy: Clinical implications, challenges and solutions for treatment resistance. Semin Cell Dev Biol 64:107–115
25. Cortese M, Torchiaro E, Leto S et al Design, characterization and preclinical validation of a combinatorial CAR-based immunotherapy against colorectal cancer with HER2 amplification. J Immunother Cancer. 2022;10. Epub ahead of print 7 November 2022. https://doi.org/10.1136/jitc-2022-SITC2022.0213
26. Halder D, Das S (2023) Role of multi-targeted bioactive natural molecules and their derivatives in the treatment of Alzheimer's disease: an insight into structure-activity relationship. J Biomol Struct Dyn 41:11286–11323
27. Maroyi A (2014) The genus Warburgia: A review of its traditional uses and pharmacology. Pharm Biol 52:378–391
28. Okello D, Komakech R, Matsabisa MG et al (2018) A review on the botanical aspects, phytochemical contents and pharmacological activities of Warburgia ugandensis. J Med Plants Res 12:448–455
29. Okello D, Kang Y (2021) Ethnopharmacological Potentials of Warburgia ugandensis on Antimicrobial Activities. Chin J Integr Med 27:633–640
30. Macharia JM, Maina JK, Zand A et al (2025) Antitumor Activity of Warbugia ugandensis: Methanolic Extracts and Gene Regulation in Colorectal Cancer. Nutrients 17:471
31. Opiyo S (2023) Warburgia ugandensis: a review of compounds and bioactivity. Int J Pharmacogn Chem 4(2):35–45. https://doi.org/10.46796/ijpc.v4i2.457
32. Chandrasekhar V, Rajan K, Kanakam SRS et al (2025) COCONUT 2.0: a comprehensive overhaul and curation of the collection of open natural products database. Nucleic Acids Res 53:D634–D643
33. Sarkar P, Alheety MA, Srivastava V (2023) Molecular Docking and ADMET Study of Spice-Derived Potential Phytochemicals against Human DNA Topoisomerase III Alpha. Macromol Symp 407:2200108
34. Gfeller D, Grosdidier A, Wirth M et al (2014) SwissTargetPrediction: a web server for target prediction of bioactive small molecules. Nucleic Acids Res 42:W32–W38
35. Daina A, Michielin O, Zoete V (2019) SwissTargetPrediction: updated data and new features for efficient prediction of protein targets of small molecules. Nucleic Acids Res 47:W357–W364
36. Stelzer G, Rosen N, Plaschkes I et al (2016) The GeneCards Suite: From Gene Data Mining to Disease Genome Sequence Analyses. Curr Protoc Bioinforma 54:1301–13033
37. Ather SH, Awe OI, Butler TJ et al SeqAcademy: an educational pipeline for RNA-Seq and ChIP-Seq analysis. Epub ahead of print 22 September 2020. https://doi.org/10.12688/f1000research.14880.4
38. Oliveros JC (2007–2015) Venny. An interactive tool for comparing lists with Venn's diagrams. Centro Nacional de Biotecnología (CNB-CSIC). https://bioinfogp.cnb.csic.es/tools/venny/index.html
39. Szklarczyk D, Kirsch R, Koutrouli M et al (2023) The STRING database in 2023: protein–protein association networks and functional enrichment analyses for any sequenced genome of interest. Nucleic Acids Res 51:D638–D646
40. El Abed F, Baraket G, Nyamari MN et al (2023) Differential expression analysis of miRNAs and mRNAs in epilepsy uncovers potential biomarkers. bioRxiv. https://doi.org/10.1101/2023.09.11.557132
41. Alaya F, Baraket G, Adediran DA et al (2024) Multiple sclerosis stages and their differentially expressed genes: a bioinformatics analysis. bioRxiv. https://doi.org/10.1101/2024.01.20.576448
42. Ben Aribi H, Abassi N, Awe OI (2024) NeuroVar: an open-source tool for the visualization of gene expression and variation data for biomarkers of neurological diseases. Gigabyte. https://doi.org/10.46471/gigabyte.143
43. Ben Aribi H, Naitore C, Ayadi F, et al (2025) EMImR: a Shiny application for identifying transcriptomic and epigenomic changes. Gigabyte. https://doi.org/10.46471/gigabyte.168
44. Tang D, Chen M, Huang X et al (2023) SRplot: A free online platform for data visualization and graphing. PLoS ONE 18:e0294236
45. He S, Wu J, Han D et al (2022) Differential expression profile of plasma exosomal microRNAs in chronic rhinosinusitis with nasal polyps. Exp Biol Med 247:1039–1046
46. Gakpey MEL, Aidoo SAA, Jumah TA et al (2025) Targeting aldose reductase using natural African compounds as promising agents for managing diabetic complications. Front Bioinform 5. Epub ahead of print 6 February 2025. https://doi.org/10.3389/fbinf.2025.1499255
47. Sonwane PN, Kumbhare MR (2025) Molecular docking and pharmacokinetics of benzimidazole-based FtsZ inhibitors for tuberculosis. Sci Rep 15:35270
48. Mbotoni MS, Nagagi YP, Shadrack DM et al (2026) Phytochemical screening, acaricidal activity, and in silico analysis of *Commiphora swynnertonii* extracts against *Rhipicephalus decoloratus* and *Rhipicephalus microplus*. J Nat Pestic Res 18:100208
49. Nandana PI, Rasyid H, Prihantono et al (2023) Molecular docking studies of Brucein D as a potential inhibitor of the Bcl-2 anti-apoptotic protein. Bali Med J 12:2148–2152
50. Makaye AI, Paul L, Vuai SAH et al (2025) In silico ligand self-assembly drives binding recognition of natural products into Anopheles gambiae cytosolic sulfotransferases (AgSULT-001425) protein. Silico Pharmacol 13:138
51. Martin DR, Mutombwera AT, Madiehe AM et al (2025) Molecular modeling and simulation studies of SELEX-derived high-affinity DNA aptamers to the Ebola virus nucleoprotein. J Biomol Struct Dyn 43:4405–4422
52. Martin DR, Ajmal A, Meyer M et al (2025) In silico identification of phytoconstituents from Capparis sepiaria as interleukin-1 inhibitors for rheumatoid arthritis: molecular docking, ADMET profiling, and molecular dynamics simulation. Silico Pharmacol 13:106
53. Martin DR, Oselusi SO, Armien A et al (2026) Computational identification of potential COX-2 inhibitors from Devil's Claw for anti-inflammation. Silico Res Biomed 2:100370
54. Fadaka AO, Sibuyi NRS, Martin DR et al (2021) Development of Effective Therapeutic Molecule from Natural Sources against Coronavirus Protease. Int J Mol Sci 22:9431
55. Li AP (2001) Screening for human ADME/Tox drug properties in drug discovery. Drug Discov Today 6:357–366
56. Dey A, Mitra A, Pathak S et al (2023) Recent Advancements, Limitations, and Future Perspectives of the use of Personalized Medicine in Treatment of Colon Cancer. Technol Cancer Res Treat 22:15330338231178403
57. Li Q, Geng S, Luo H et al (2024) Signaling pathways involved in colorectal cancer: pathogenesis and targeted therapy. Signal Transduct Target Ther 9:266
58. Fang J, Liu C, Wang Q et al (2018) In silico polypharmacology of natural products. Brief Bioinform 19:1153–1171
59. Yang X-LCRC, Platform A colorectal cancer domain-specific chemogenomics knowledgebase for polypharmacology and target identification research. 2015. https://www.semanticscholar.org/paper/CRC-Platform%3A-A-Colorectal-Cancer-Domain-specific-Yang/e6f85a7bfb5bbfc396eb5379ce15f1a5248ded1e. accessed 16 June 2026
60. Almatroudi A, Allemailem KS, Alwanian WM et al (2023) Effects and Mechanisms of Kaempferol in the Management of Cancers through Modulation of Inflammation and Signal Transduction Pathways. Int J Mol Sci 24:8630
61. Dubey N, Dubey N, Bhadoria U et al (2023) Targeting colorectal cancer using dietary flavonols. Cancer Innov 3:e99
62. Refolo MG, D'Alessandro R, Malerba N et al (2015) Anti Proliferative and Pro Apoptotic Effects of Flavonoid Quercetin Are Mediated by CB1 Receptor in Human Colon Cancer Cell Lines. J Cell Physiol 230:2973–2980
63. Dharani NA Review of phytochemical constituents and pharmacological activities of ethnomedicinal Warburgia ugandensis Sprague ssp. ugandensis in East Africa. 2020. https://journaluploads.psk.or.ke/Vol.24%20No3%20man%204.pdf. accessed 16 June 2026
64. Darband SG, Kaviani M, Yousefi B et al (2018) Quercetin: A functional dietary flavonoid with potential chemo-preventive properties in colorectal cancer. J Cell Physiol 233:6544–6560
65. Li Q, Wei L, Lin S et al (2019) Synergistic effect of kaempferol and 5–fluorouracil on the growth of colorectal cancer cells by regulating the PI3K/Akt signaling pathway. Mol Med Rep 20:728–734
66. Uttarawichien T, Kamnerdnond C, Inwisai T et al (2021) Quercetin Inhibits Colorectal Cancer Cells Induced-Angiogenesis in Both Colorectal Cancer Cell and Endothelial Cell through Downregulation of VEGF-A/VEGFR2. Sci Pharm 89:23
67. Wu H, Du J, Li C et al (2022) Kaempferol Can Reverse the 5-Fu Resistance of Colorectal Cancer Cells by Inhibiting PKM2-Mediated Glycolysis. Int J Mol Sci 23:3544
68. Dwivedi PSR, Bharathi AM, Lobo WL et al (2026) Network pharmacology and computational dissection of Solanum trilobatum bioactives reveals modulation of steroid receptor associated signalling in breast cancer. Beni-Suef Univ J Basic Appl Sci 15:29
69. Gu C, Tang L, Hao Y et al (2023) Network pharmacology and bioinformatics were used to construct a prognostic model and immunoassay of core target

genes in the combination of quercetin and kaempferol in the treatment of colorectal cancer. J Cancer 14:1956–1980
70. Enejoh OA, Okonkwo CH, Nortey H et al Machine learning and molecular dynamics simulations predict potential TGR5 agonists for type 2 diabetes treatment. Front Chem. 2025;12. Epub ahead of print 9 January 2025. https://doi.org/10.3389/fchem.2024.1503593
71. Gakpey MELEL, Aidoo SAA, Jumah TA et al Targeting aldose reductase using natural African compounds as promising agents for managing diabetic complications. Front Bioinforma. 2025;5. Epub ahead of print 6 February 2025. https://doi.org/10.3389/fbinf.2025.1499255
72. Hanson G, Adams J, Kepgang DIB et al Machine learning and molecular docking prediction of potential inhibitors against dengue virus. Front Chem. 2024;12. Epub ahead of print 24 December 2024. https://doi.org/10.3389/fchem.2024.1510029
73. Die JV, Elmassry MM, LeBlanc KH, Awe OI, Dillman A, Busby B (2019) geneHummus: an R package to define gene families and their expression in legumes and beyond. BMC Genomics 20:591. https://doi.org/10.1186/s12864-019-5952-2
74. Zhang H, Tang J, Cao H et al (2025) Effect and mechanism of *Magnolia officinalis* in colorectal cancer: Multi-component-multi-target approach. J Ethnopharmacol 338:119007
75. Jin W (2020) Regulation of Src Family Kinases during Colorectal Cancer Development and Its Clinical Implications. Cancers 12:1339
76. Li J, Li Z, Cui M et al (2025) Drimartol B, a sesquiterpene coumarin of the edible powder of *Artemisia sphaerocephala* seed, induced apoptosis in NSCLC cells via PI3K/AKT/FoxO3a pathway inhibition. J Funct Foods 124:106646
77. Yan L, Shi J, Zhu J (2024) Cellular and molecular events in colorectal cancer: biological mechanisms, cell death pathways, drug resistance and signalling network interactions. Discov Oncol 15:294
78. Mikkili I, Suluvoy JK, Thathapudi JJ et al (2024) Synergistic strategies for cancer treatment: leveraging natural products, drug repurposing and molecular targets for integrated therapy. Beni-Suef Univ J Basic Appl Sci 13:96
79. Mu B-X, Li Y, Ye N et al (2024) Understanding apoptotic induction by *Sargentodoxa cuneata-Patrinia villosa* herb pair via PI3K/AKT/mTOR signalling in colorectal cancer cells using network pharmacology and cellular studies. J Ethnopharmacol 319:117342
80. Tripathi PK, Jain CK (2025) Unravelling phyto-compound therapeutics against colorectal cancer: targeting SRC proto-oncogene via fibroblast growth factor signalling pathway —a comprehensive approach integrating omics data analysis, network pharmacology, virtual screening, and molecular dynamics. Recent Adv Food Nutr Agric 16:185–205
81. Zheng Q, Wang X, Gao T et al (2023) Exploring the pharmacological and molecular mechanisms of Salvia chinensis Benth in colorectal cancer: A network pharmacology and molecular docking study. Med (Baltim) 102:e36602
82. Liang B, Li C, Zhao J (2016) Identification of key pathways and genes in colorectal cancer using bioinformatics analysis. Med Oncol 33:111
83. Danielsen SA, Eide PW, Nesbakken A et al (2015) Portrait of the PI3K/AKT pathway in colorectal cancer. Biochim Biophys Acta BBA - Rev Cancer 1855:104–121
84. Hou X, Ren C, Jin J et al (2025) Phosphoinositide signalling in cell motility and adhesion. Nat Cell Biol 27:736–748
85. Oh B-C (2023) Phosphoinositides and intracellular calcium signaling: novel insights into phosphoinositides and calcium coupling as negative regulators of cellular signaling. Exp Mol Med 55:1702–1712
86. Kang D, Li J, Li Y et al (2025) Prognostic significance of KRAS, NRAS, BRAF, and PIK3CA mutations in stage II/III colorectal cancer: A retrospective study and meta-analysis. PLoS ONE 20:e0320783
87. Wu J-B, Li X-J, Liu H et al (2023) Association of KRAS, NRAS, BRAF and PIK3CA gene mutations with clinicopathological features, prognosis and ring finger protein 215 expression in patients with colorectal cancer. Biomed Rep 19:1–15
88. Capraro D, Connor DE, Joseph JE (2026) Investigating the effects of platelets, platelet releasate and aspirin on colorectal cancer cell proliferation, migration and invasion. Med Oncol 43:144
89. Contursi A, Fullone R, Szklanna-Koszalinska P et al (2023) Tumor-Educated Platelet Extracellular Vesicles: Proteomic Profiling and Crosstalk with Colorectal Cancer Cells. Cancers 15:350
90. Broszkiewicz W, Domińska K (2025) The role of relaxins in blood cell modulation: interactions with relaxin family peptide receptor 1 (RXFP1) and glucocorticoid receptor (GR). Clin Sci 139:1431–1450
91. Hu T, Li LF, Shen J et al (2015) Chronic Inflammation and Colorectal Cancer: The Role of Vascular Endothelial Growth Factor. Curr Pharm Des 21:2960–2967
92. Jung J, Han H The diverse influences of relaxin-like peptide family on tumor progression: Potential opportunities and emerging challenges. Heliyon. 2024;10. Epub ahead of print 30 January 2024. https://doi.org/10.1016/j.heliyon.2024.e24463
93. Kotwal A, Goldner WS, Bennett RG (2024) Role of Relaxin Signaling in Cancer: A Review. Biochem Pharmacol 230:116634
94. Bordelon CL, Stephens JM (2026) Lipolysis in Health and Disease: Pathways, Regulation, and Metabolic Consequences. Curr Diab Rep 26:8
95. Morigny P, Houssier M, Mouisel E et al (2016) Adipocyte lipolysis and insulin resistance. Biochimie 125:259–266
96. Yagyu H, Kiuchi M, Sasaki A et al (2025) Lipolysis-microlipophagy cascade regulated by adipose triglyceride lipase drives pathogenic adaptive type 2 immunity. Sci Immunol 10:eadp0849
97. Kim SH, Park JG, Lee J et al (2015) The Dietary Flavonoid Kaempferol Mediates Anti-Inflammatory Responses via the Src, Syk, IRAK1, and IRAK4 Molecular Targets. Mediators Inflamm 2015:904142
98. Lomphithak T, Jaikla P, Sae-Fung A et al (2023) Natural Flavonoids Quercetin and Kaempferol Targeting G2/M Cell Cycle-Related Genes and Synergize with Smac Mimetic LCL-161 to Induce Necroptosis in Cholangiocarcinoma Cells. Nutrients 15:3090
99. Pantsar T, Poso A (2018) Binding Affinity via Docking: Fact and Fiction. Molecules 23:1899
100. Chda A, Bencheikh R (2023) Flavonoids as G Protein-coupled Receptors Ligands: New Potential Therapeutic Natural Drugs. Curr Drug Targets 24:1346–1363
101. Zughaibi TA, Suhail M, Tarique M et al (2021) Targeting PI3K/Akt/mTOR Pathway by Different Flavonoids: A Cancer Chemopreventive Approach. Int J Mol Sci 22:12455
102. Gautam G Advancement of network pharmacology in multi-targeted therapeutic evaluation of medicinal plants. J CAM Res Prog. 2023;1. Epub ahead of print 2023. https://doi.org/10.33790/jcrp1100113
103. Sharma B, Yadav DK (2022) Metabolomics and Network Pharmacology in the Exploration of the Multi-Targeted Therapeutic Approach of Traditional Medicinal Plants. Plants 11:3243
104. Iranshahi M, Barthomeuf C, Bayet-Robert M et al (2014) Drimane-Type Sesquiterpene Coumarins from Ferula gummosa Fruits Enhance Doxorubicin Uptake in Doxorubicin-Resistant Human Breast Cancer Cell Line. J Tradit Complement Med 4:118–125
105. Sak K (2014) Characteristic Features of Cytotoxic Activity of Flavonoids on Human Cervical Cancer Cells. Asian Pac J Cancer Prev 15:8007–8018
106. Selvakumar P, Badgeley A, Murphy P et al (2020) Flavonoids and Other Polyphenols Act as Epigenetic Modifiers in Breast Cancer. Nutrients 12:761
107. Zheng W, Han L, He Z-J et al (2024) Novel drimane-type sesquiterpenoids and nucleosides from the Helicoma septoconstrictum suppress the growth of ovarian cancer cells. Bioorg Chem 145:107214
108. Liu K, Watanabe E, Kokubo H (2017) Exploring the stability of ligand binding modes to proteins by molecular dynamics simulations. J Comput Aided Mol Des 31:201–211
109. Gomes BS, Simões B, Mendes PM (2018) The increasing dynamic, functional complexity of bio-interface materials. Nat Rev Chem 2:0120
110. Fu M, Gao L, Geng Q et al (2023) Noncovalent interaction mechanism and functional properties of flavonoid glycoside-β-lactoglobulin complexes. Food Funct 14:1357–1368
111. Menéndez CA, Accordino SR, Gerbino DC et al (2016) Hydrogen Bond Dynamic Propensity Studies for Protein Binding and Drug Design. PLoS ONE 11:e0165767
112. Huang K, Luo S, Cong Y et al (2020) An accurate free energy estimator: based on MM/PBSA combined with interaction entropy for protein–ligand binding affinity. Nanoscale 12:10737–10750
113. Deganutti G, Moro S (2017) Estimation of Kinetic and Thermodynamic Ligand-Binding Parameters Using Computational Strategies. Future Med Chem 9:507–523
114. Zhou H-X, Gilson MK (2009) Theory of Free Energy and Entropy in Noncovalent Binding. Chem Rev 109:4092–4107
115. Ahalawat N, Sahil M, Mondal J (2023) Resolving Protein Conformational Plasticity and Substrate Binding via Machine Learning. J Chem Theory Comput 19:2644–2657

116. Dornan GL, Siempelkamp BD, Jenkins ML et al (2017) Conformational disruption of PI3Kδ regulation by immunodeficiency mutations in PIK3CD and PIK3R1. Proc Natl Acad Sci U S A 114:1982–1987
117. El-Kattan A, Varma M Oral, absorption intestinal metabolism and human oral bioavailability. In: Topics on drug metabolism. IntechOpen. Epub ahead of print 22 February 2012. https://doi.org/10.5772/31087
118. Nguyen T-T-L, Duong V-A, Maeng H-J (2021) Pharmaceutical Formulations with P-Glycoprotein Inhibitory Effect as Promising Approaches for Enhancing Oral Drug Absorption and Bioavailability. Pharmaceutics 13:1103
119. Mohan Kumar D, Talwar P Neurotherapeutics across blood–brain barrier: screening of BBB-permeable and CNS-active molecules for neurodegenerative disease. Front Pharmacol. 2025;16. Epub ahead of print 26 September 2025. https://doi.org/10.3389/fphar.2025.1616144
120. Sert Y (2025) Pharmacokinetic Evaluation of Sulfadicramide through SwissADME: A Computational Insight into Drug-Likeness and Bioavailability. MAS J Appl Sci 10:357–362
121. Farouk F, Shamma R (2019) Chemical structure modifications and nanotechnology applications for improving ADME-Tox properties, a review. Arch Pharm (Weinheim) 352:1800213
122. Kitte R, Tretbar M, Dluczek S et al (2021) Chemical and Cytotoxic Activity of three main Sesquiterpenoids from *Warburgia ugandensis*. Results Chem 3:100242

Publisher's note

Springer Nature remains neutral with regard to jurisdictional claims in published maps and institutional affiliations.